NASA Tech Briefs

National Aeronautics and
Space Administration

Electronic Components and Circuits

Electronic Systems

Physical Sciences

Materials

Computer Programs

Mechanics

Machinery

Fabrication Technology

Mathematics and Information Sciences

Life Sciences

INTRODUCTION

Tech Briefs are short announcements of innovations originating from research and development activities of the National Aeronautics and Space Administration. They emphasize information considered likely to be transferable across industrial, regional, or disciplinary lines and are issued to encourage commercial application.

Availability of NASA Tech Briefs and TSPs

Requests for individual Tech Briefs or for Technical Support Packages (TSPs) announced herein should be addressed to

National Technology Transfer Center
Telephone No. **(800) 678-6882** or via World Wide Web at **www2.nttc.edu/leads/**

Please reference the control numbers appearing at the end of each Tech Brief. Information on NASA's Commercial Technology Team, its documents, and services is also available at the same facility or on the World Wide Web at **www.nctn.hq.nasa.gov**.

Commercial Technology Offices and Patent Counsels are located at NASA field centers to provide technology-transfer access to industrial users. Inquiries can be made by contacting NASA field centers and program offices listed below.

NASA Field Centers and Program Offices

Ames Research Center
Carolina Blake
(650) 604-0893 or
cblake@mail.arc.nasa.gov

Dryden Flight Research Center
Lee Duke
(805) 258-3802 or
lee.duke@dfrc.nasa.gov

Goddard Space Flight Center
George Alcorn
(301) 286-5810 or
galcorn@gsfc.nasa.gov

Jet Propulsion Laboratory
Merle McKenzie
(818) 354-2577 or
merle.mckenzie@comail.jpl.nasa.gov

Johnson Space Center
Hank Davis
(281) 483-0474 or
hdavis@gp101.jsc.nasa.gov

John F. Kennedy Space Center
Gale Allen
(407) 867-6626 or
galeallen-1@ksc.nasa.gov

Langley Research Center
Dr. Joseph S. Heyman
(804) 864-6006 or
j.s.heyman@larc.nasa.gov

Glenn Research Center
Larry Viterna
(216) 433-3484 or
cto@lerc.nasa.gov

George C. Marshall Space Flight Center
Sally Little
(256) 544-4266 or
sally.little@msfc.nasa.gov

John C. Stennis Space Center
Kirk Sharp
(228) 688-1929 or
ksharp@ssc.nasa.gov

NASA Program Offices
At NASA Headquarters there are seven major program offices that develop and oversee technology projects of potential interest to industry:

Carl Ray
Small Business Innovation Research Program (SBIR) & Small Business Technology Transfer Program (STTR)
(202) 358-4652 or
cray@mail.hq.nasa.gov

Dr. Robert Norwood
Office of Aeronautics and Space Transportation Technology (Code R)
(202) 358-2320 or
rnorwood@mail.hq.nasa.gov

John Mulcahy
Office of Space Flight (Code MP)
(202) 358-1401 or
jmulcahy@mail.hq.nasa.gov

Gerald Johnson
Office of Aeronautics (Code R)
(202) 358-4711 or
g_johnson@aeromail.hq.nasa.gov

Bill Smith
Office of Space Science (Code S)
(202) 358-2473 or
wsmith@sm.ms.ossa.hq.nasa.gov

Roger Crouch
Office of Microgravity Science Applications (Code U)
(202) 358-0689 or
rcrouch@hq.nasa.gov

Granville Paules
Office of Mission to Planet Earth (Code Y)
(202) 358-0706 or
gpaules@mtpe.hq.nasa.gov

BLANK PAGE

NASA TechBriefs

National Aeronautics and Space Administration

July 1999
99-07

BLANK PAGE

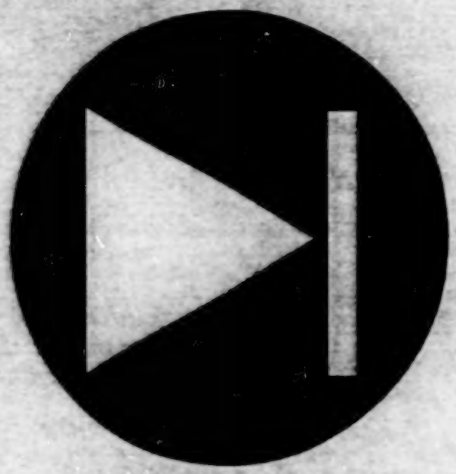

Electronic Components and Circuits

Hardware, Techniques, and Processes

BLANK PAGE

Series-Connected Boost Regulators

Dc-to-dc converters serve as building blocks of modular electric-power systems.

John H. Glenn Research Center, Cleveland, Ohio

A series-connected boost regulator (SCBR) is, as its name suggests, an electronic circuit for boosting a power-supply voltage to a higher and regulated value. The distinguishing feature of an SCBR is an interconnection topology in which one utilizes the input/output dc-isolating quality of a dc-to-dc converter. (Other, similar terms that have been used to denote an SCBR include "series-connected converter," "series-connected boost converter," and "series-connected boost unit.")

SCBRs were conceived as building blocks of relatively inexpensive, modular power-management-and-distribution (PMAD) systems for future spacecraft. Potential terrestrial applications for the SCBR concept include output regulators and storage-battery chargers for solar photovoltaic arrays.

The top part of Figure 1 is a simplified schematic diagram of a typical dc-to-dc power converter, showing how dc isolation between the input and output sides is achieved by use of transformer coupling. The bottom part of Figure 1 illustrates the utilization of the same dc-to-dc converter in a basic SCBR, in which one connects the input "hot" terminal to the output return ("cold") terminal; in effect, the input and output are connected in series, so that their voltages add to yield a higher overall output voltage.

An important advantage afforded by an SCBR is the ability to use a dc-to-dc converter to regulate more power than it is rated to handle by itself, at an overall efficiency greater than that of the dc-to-dc converter by itself. Figure 2 illustrates the example of an SCBR that supplies a regulated potential of 28 Vdc to a load of 2.8 Ω (thus supplying a load current of 10 A). In this example, the available power-supply potential is 20 Vdc (unregulated), and one uses a dc-to-dc converter as a boost regulator to increase the load potential to the desired regulated 28 Vdc.

The dc-to-dc converter considered by itself is rated to put out a current of 10 A at a potential of 8 Vdc (thus, an output power of 80 W) while drawing an input current of 4.7 A at the supply potential of 20 Vdc (thus, an input power of 94 W). Under these conditions, its efficiency (output power ÷ input power) is about 85 percent.

However, the dc-to-dc converter does not operate by itself. With respect to the load current, it is connected in series with the 20-Vdc power supply. As a consequence, it processes only a fraction of the total regulated power of 280 W delivered to the load; this is the sense in which the dc-to-dc converter can be regarded as regulating more power than it is rated to handle by itself.

The current drawn from the 20-Vdc power supply in this example is 14.7 A, comprising the load current of 10 A and the 4.7-A input current for the dc-to-dc converter. The total power consumed is thus 20 × 14.7 = 294 W. Then the overall efficiency (regulated output power ÷ total power consumed) is about 95 percent, which is greater than the efficiency of the dc-to-dc converter considered by itself.

SCBRs can be built at relatively low cost because dc-to-dc converters are commercially available and relatively inexpensive. A basic SCBR can be used by itself or in combination with other building blocks (including other SCBRs). Other advantages of SCBRs include high power densities, adaptability to positive-ground power systems, and capabilities for high degrees of fault tolerance.

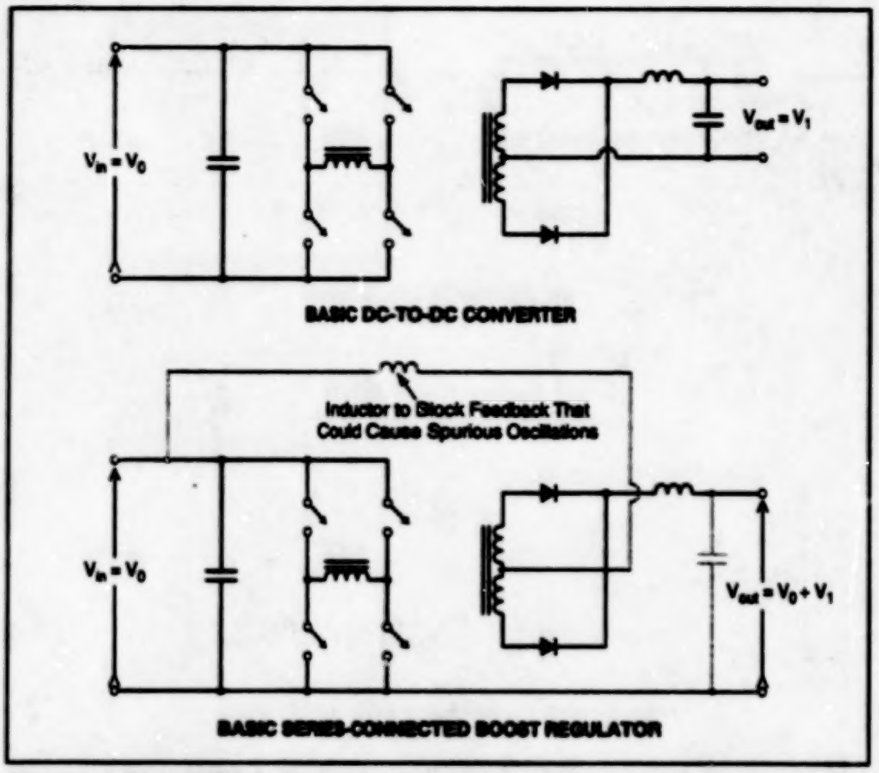

Figure 1. A Basic SCBR Is Formed by connecting the "hot" terminal on the input side of a dc-to-dc converter to the return ("cold") terminal on its output side.

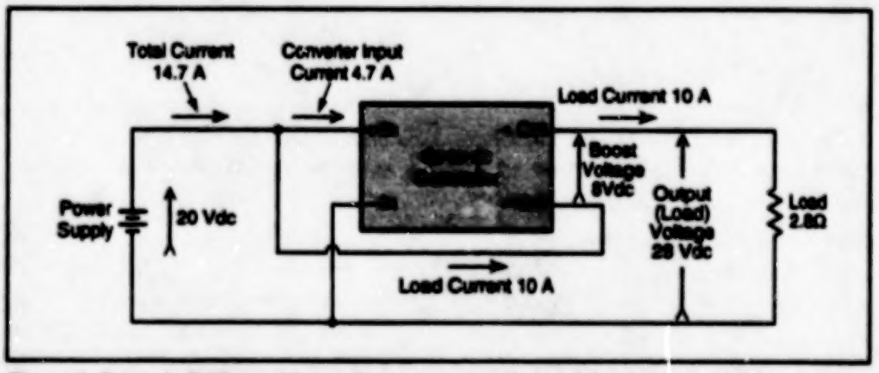

Figure 2. Power Is Delivered from a 20-V power supply to a 2.8-Ω load via an 8-V-output dc-to-dc converter connected and operated as a boost regulator.

This work was done by Raymond F. Beach and Robert Button of Glenn Research Center and Andy Brush of Sverdrup Technology, Inc. Further information is contained in a TSP [see page 1].

Inquiries concerning rights for the commercial use of this invention should be addressed to NASA Glenn Research Center, Commercial Technology Office, Attn: Tech Brief Patent Status, Mail Stop 7–3, 21000 Brookpark Road, Cleveland, Ohio 44135. Refer to LEW-15918.

Improved Q-Switch Drivers

Single or multiple fast-rise, long-duration voltage pulses can be produced.

Langley Research Center, Hampton, Virginia

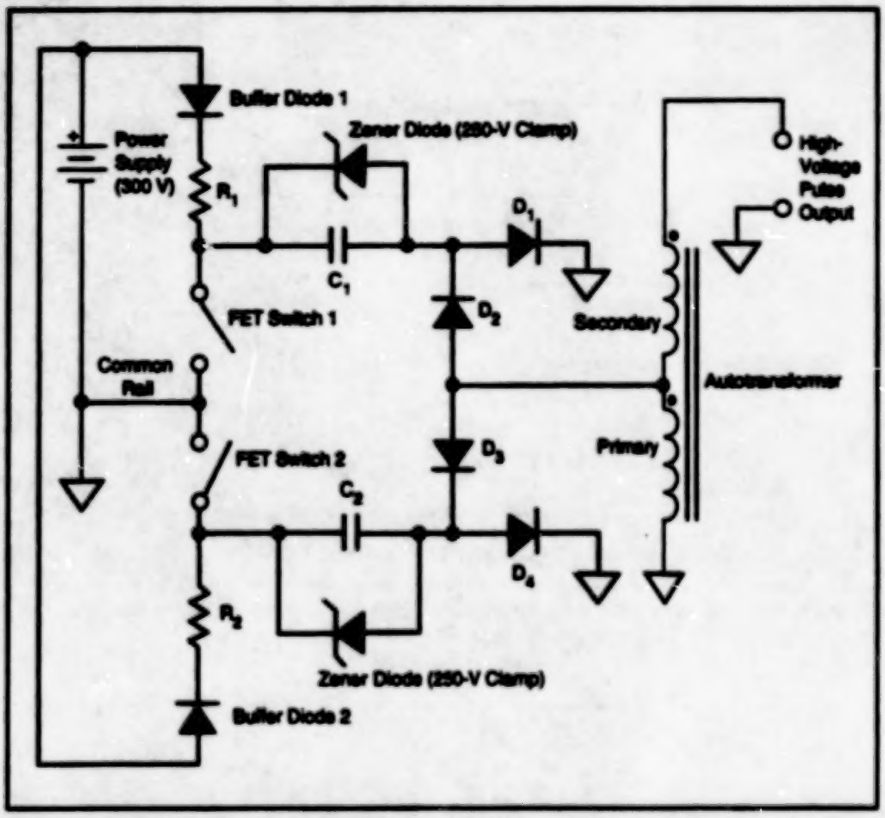

Either Capacitor Can Be Discharged into the transformer without discharging the other. They can be discharged in rapid succession to produce two rapid-rise, long-duration Q-switch pulses.

Improved circuits that generate high-voltage pulses for driving Q-switched lasers have been devised. To extract maximum energy from a laser cavity in the form of consistent laser pulses, the Q-switch pulses must rise rapidly so that the Q-switch is fully open before each laser pulse occurs. The Q-switch drivers placed in use heretofore generate high-voltage pulses that rise rapidly enough to accommodate the short laser-pulse-evolution times, but many conventional Q-switch drivers produce high-voltage pulses which are so short that accurate timing is needed to ensure that the laser pulses occur while the Q-switches are fully open. The timing problem is compounded, and thus the range of usable operating conditions reduced, by the variability of the laser-pulse-evolution time with variations in the storage and loss of laser-pumping energy.

The improved Q-switch drivers provide fast-rising, nearly square high-voltage pulses that last long enough (typically about 300 ns) to accommodate a wider range of laser-pulse-evolution times, thereby making timing much less critical and enabling lasers to function more reliably and at higher efficiency over wider ranges of operating conditions. In addition, the improved circuits can generate multiple high-voltage pulses in rapid succession.

A driver circuit of this type generates a high-voltage pulse by discharging a capacitor through a step-up autotransformer designed specifically for the required pulse operation. Long-duration pulses are achieved by selection of a toroidal ferrite transformer core that has a relative magnetic permeability of 3,000, by choice of the dimensions of the core, and by optimizing the numbers of turns (at a turns ratio of 8) and configurations of the primary and secondary windings.

The figure is a simplified schematic diagram of the charging and discharging circuits in an improved Q-switch driver that can generate two pulses in rapid succession. Capacitors C_1 and C_2 are charged from a power supply (typically +300 V); to promote consistent charging from shot to shot and to shorten the charging time, the voltage on each of these capacitors is clamped, by a zener diode, at a value (typically 250 V) less than that of the power supply. Diodes D_2 and D_3 are part of an energy-steering network through which both C_1 and C_2 are connected to the single autotransformer and through which either capacitor can be discharged into the transformer without discharging the other. Diodes D_1 and D_4 act as clippers, preventing overshoot and suppressing ringing to make the output pulses more nearly square.

Single- or dual-pulse operation can be selected by use of control logic circuitry (not shown). The discharge path of each capacitor passes through a field-effect-transistor (FET) switch, which initiates discharge by connecting the positively charged terminal of the capacitor to the common power-supply rail (in essence, ground). To speed the charging of the input capacitance of the FET and thereby make the discharge pulse rise rapidly, the turn-on pulse is supplied to the gate of each FET through a dedicated low-impedance, transformer-coupled input circuit.

This work was done by Norman P. Barnes of Langley Research Center and Charles Nichols of Hughes STX Corp.
LAR-14803

Improved Successive-Approximation ADCs With Charge Balancing

Charge balancing is effected by single self-cascoded inverters.

NASA's Jet Propulsion Laboratory, Pasadena, California

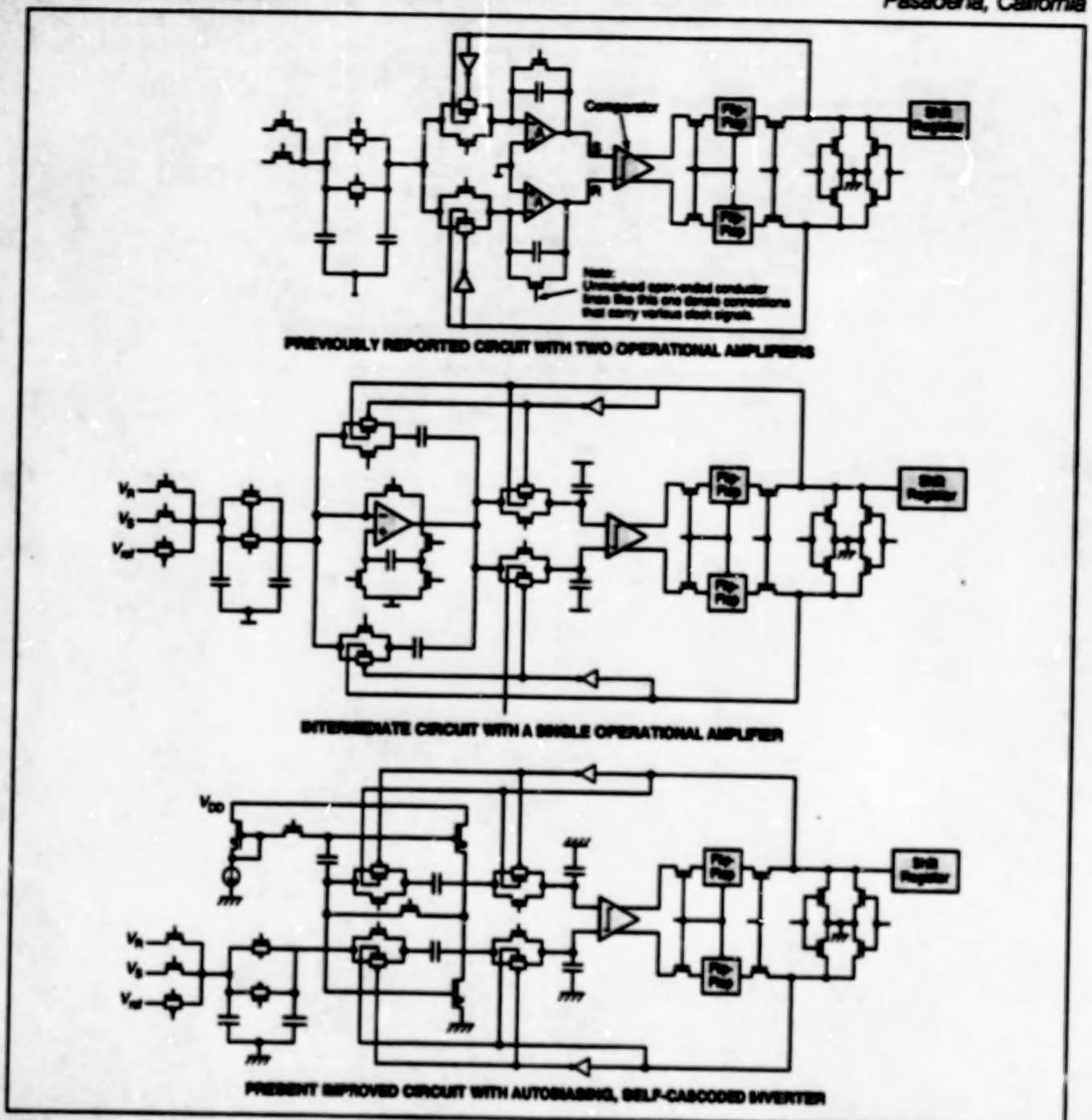

The Present Improved ADC with a single simple inverter is derived from a previously reported charge-balancing ADC with two charge-integrating operational amplifiers via an intermediate version with one operational amplifier.

Improved successive-approximation analog-to-digital converter (ADC) circuits are undergoing development for eventual incorporation into focal-plane arrays of photodetectors. These circuits are derived from, and offer advantages over, the ones described in "Successive-Approximation ADCs With Charge Balancing" (NPO-19784), *NASA Tech Briefs*, Vol. 21, No. 5 (May 1997), page 47.

The top part of the figure, shows a circuit of the previously reported type. The circuit implements successive-approximation analog-to-digital conversion according to a charge-balancing approach, in which the reset (R) and signal (S) branches of the circuit accumulate successively halved increments of reference charge in an attempt to balance the charges in the two branches. The circuit includes two high-gain charge-integrating operational amplifiers, the components of which must be closely matched to achieve accuracy in conversion. To achieve close matching, it is necessary to make the transistors in the amplifiers larger and to use dc bias currents larger than one would otherwise be inclined to do; as a

consequence, the size and power consumption of the circuit are increased, making it more difficult to integrate the circuit into a high-performance focal-plane array of photodetector readout circuits.

The middle part of the figure shows a circuit at an intermediate stage of development, in which a single operational amplifier (instead of two high-gain operational amplifiers) is used to integrate charges on both the R and S branches during nonoverlapping clock phases. Sharing of the same operational amplifier by both branches results in perfect matching of dc gain and dc offset, and in a large reduction of a component of ADC error associated with dc gain. However, the error caused by the matched dc offset is not necessarily small when the dc gain is low, which it can well be in some designs.

It turns out that the offset effect can be eliminated by replacing the single operational amplifier with a single autobiasing inverter. A dc gain of 40 dB is sufficient for 8-bit accuracy, and gain greater than 40 dB can be achieved via self-cascoding of the inverter transistors. The bottom part of the figure illustrates the resulting improved ADC circuit. In comparison with a circuit of the previously reported type, a circuit of the present type can be made to operate at the same rate and the same level of accuracy while occupying less space and consuming less power.

This work was done by Zhimin Zhou and Bedabrata Pain of Caltech for **NASA's Jet Propulsion Laboratory.** *Further information is contained in a TSP [see page 1].*

In accordance with Public Law 96-517, the contractor has elected to retain title to this invention. Inquiries concerning rights for its commercial use should be addressed to

Technology Reporting Office
JPL
Mail Stop 122-116
4800 Oak Grove Drive
Pasadena, CA 91109
(818) 354-2240

Refer to NPO-19979, volume and number of this NASA Tech Briefs issue, and the page number.

Seven-Element Circularly Polarized Patch Antenna

Commercial terrestrial applications have recently been found for a spacecraft antenna.

John H. Glenn Research Center, Cleveland, Ohio

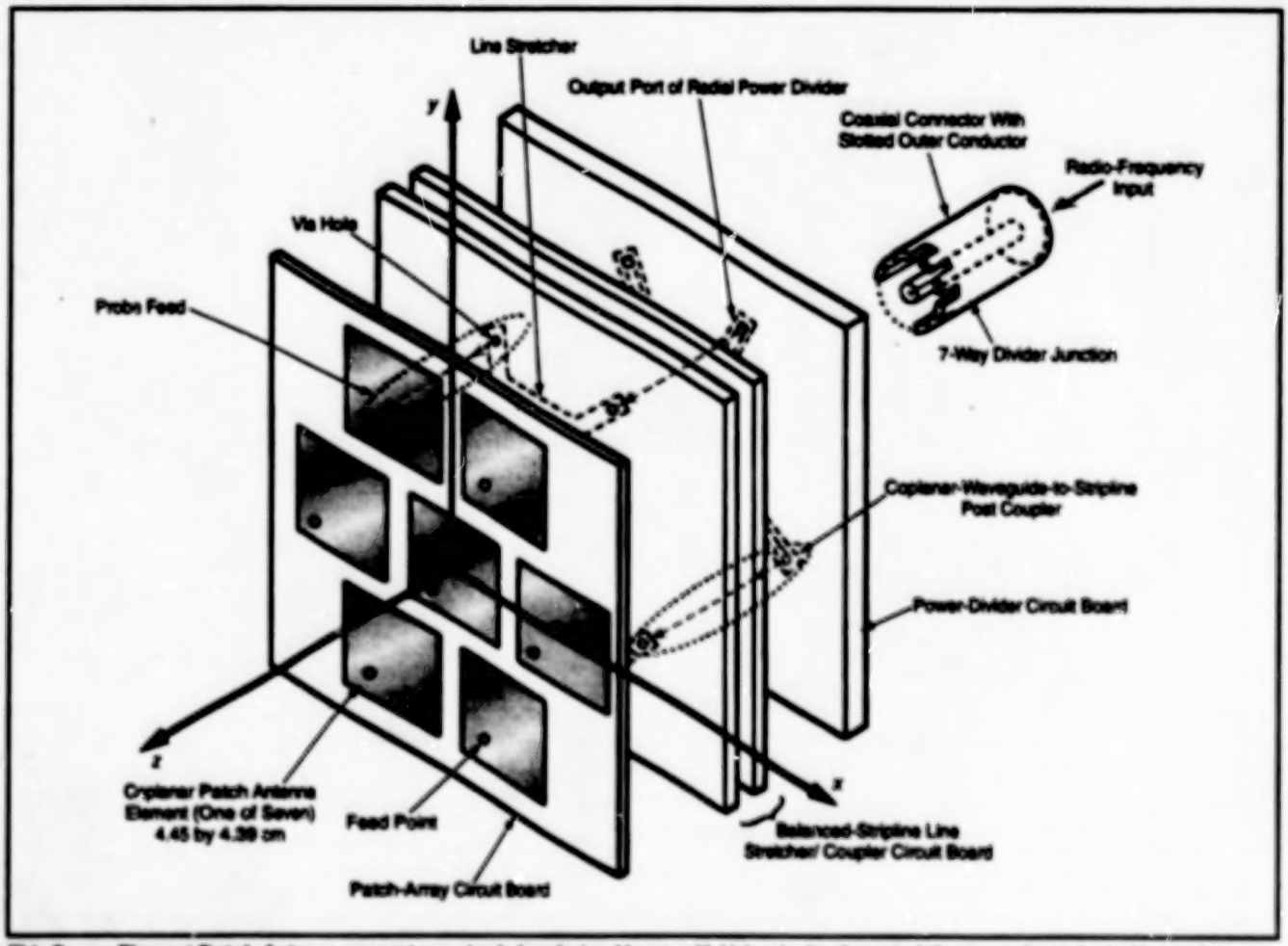

This Seven-Element Patch Antenna generates a circularly polarized beam with high gain. Its characteristics are well matched with requirements for commercial communication systems that operate at frequencies around 2.4 GHz.

A seven-element microstrip patch antenna is designed to operate with circular polarization and high gain at a frequency of 2.2875 GHz. The antenna was developed in the early 1990s as a potential replacement for a helical antenna aboard the Advanced Tracking and Data Relay Satellite. Recently, the Federal Communications Commission allocated frequencies around 2.4 GHz for commercial communication systems. The present antenna is well suited for these systems, not only

because it provides high gain in the desired frequency range, but also because like other patch antennas, it is lightweight, can be fabricated easily, can be mounted with a low profile, and is inexpensive. In addition, its circular polarization is especially advantageous in cellular-telephone and mobile communications, in that circular polarization can mitigate multipath fading, which is severe in urban environments.

The seven patch antenna elements are arranged in a hexagonal pattern (see figure). The patches are fed in equal amplitude and phase by a multilayer feed network that consists largely of coplanar-waveguide (CPW) and balanced stripline components fabricated at low cost by printed-circuit techniques.

Radio-frequency power from a transmitter is fed to the antenna through a coaxial cable that terminates in a coaxial connector. The coaxial connector is orthogonal to the plane of a seven-way radial CPW power divider. The inner conductor of the coaxial connector meets the junction formed by the middle strip conductors of the CPWs. The outer conductor of the coaxial connector is slotted and meets the ground-plane conductors of the CPW.

Each of the seven output ports of the power divider is connected, via a post coupler, to one of the ports of a balanced stripline line stretcher, which equalizes the signal-propagation path lengths to the seven patch antenna elements. Each port of the line stretcher is connected to one of the patch antenna elements by a post coupler that also serves as a probe feed.

The measured on-axis axial ratio (that is, the ratio between axes of the polarization ellipse) is 1.5 dB; in other words, the polarization is nearly circular as intended. The measured beam widths are 36° in two orthogonal meridional planes, and the gain of the antenna as determined from the beam widths is 13 dB. The measured return loss at the coaxial connector is more than 15 dB at the design frequency.

This work was done by R. Q. Lee of Glenn Research Center, G.R. Lindemood of the University of Akron, and R. N. Simons of Sverdrup Technology, Inc. Further information is contained in a TSP [see page 1].

Inquiries concerning rights for the commercial use of this invention should be addressed to NASA Glenn Research Center, Commercial Technology Office, Attn: Steve Fedor, Mail Stop 4–8, 21000 Brookpark Road, Cleveland, Ohio 44135. Refer to LEW-16713.

MMIC Converters for K- and Ka-Band Communications

Prototypes show promise for high performance and mass-producibility at low cost.

John H. Glenn Research Center, Cleveland, Ohio

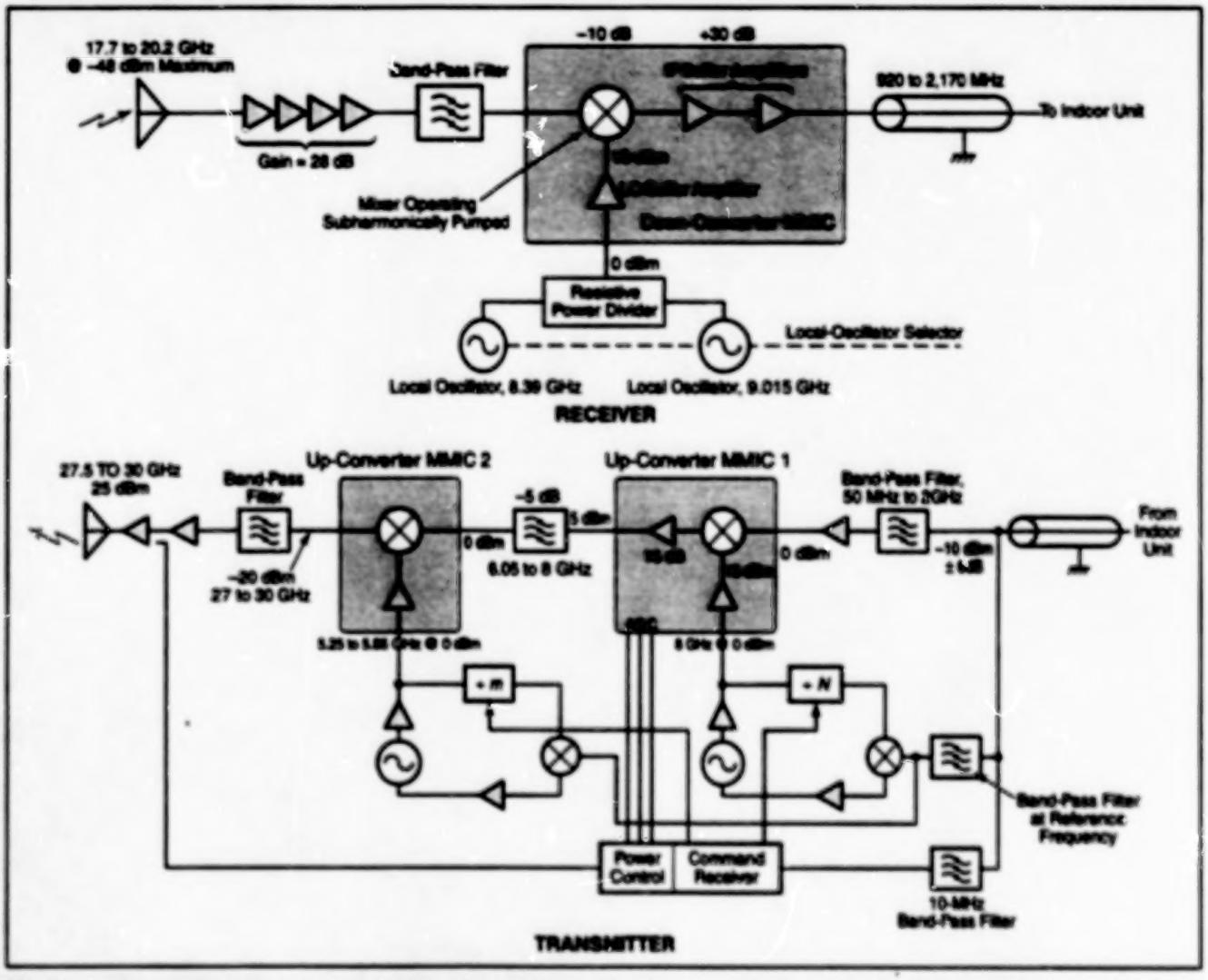

The Transmitter and Receiver at a ground station of a typical ground/satellite communication system would be contained in an outdoor unit mounted adjacent to the antenna. The receiver and transmitter would contain converters of the type developed in this program.

Monolithic microwave integrated-circuit (MMIC) frequency converters have been developed for use in satellite- and ground-based communications (see figure) at frequencies from about 18 to about 30 GHz. These and similar converters can be expected to exert significant effects on the sizes, costs, and performances of terminals for the next generation of K- and Ka-band communication systems. The rapid increase in the number of such systems is expected to give rise to a demand for tens of millions of frequency converters during the next few years.

The emphasis in this development program was on low cost, and the technical approach involved reliance on well-established design practices and mature, commercially available processes for fabrication of MMIC chips. The practices and processes selected were those of GaAs metal/semiconductor field-effect transistors (MESFETs) with 1/2-μm design rules.

The converters are capable of operation as both up- and down-converters, and are passive in the sense that external local oscillators (LOs) must be provided. Some of the converters are designed for use with subharmonic LOs, taking advantage of the decrease in cost and increase in availability of oscillators with decreasing frequency.

Some of the converters contain integrated buffer amplifiers for the LO and intermediate-frequency (IF) signals of several gigahertz, as in the example of Figure 1. However, a fundamental limitation on the range of operating frequencies of 1/2-μm MESFET amplifiers precluded the integration, into the converters, of radio-frequency (RF) amplifiers operating at frequencies from 20 to 30 GHz. As a first step in an effort to overcome this limitation, the developers fabricated a set of advanced MMICs for converters and amplifiers, using an acceptor-doped high-electron-mobility transistor (p-HEMT) design and process. It is anticipated that as the p-HEMT art matures, p-HEMT devices will offer a potential to manufacture inexpensive, highly integrated chips.

The performance of an MMIC chip can be altered by its surroundings. Factors that can affect performance include box resonances, coupling to walls, and transmission-line effects on bonding wires. Therefore, considerable attention was given to packaging. Two alternatives to conventional MMIC packaging were considered: One involved the use of a low-temperature cofired ceramic. The other involved a ball-grid-array package, which is a leadless ceramic package in surface-mount configuration with noncollapsing balls made of a copper/silver eutectic alloy.

Results of tests have shown that the up- and down-converters and p-HEMT devices perform well enough to be useful in ground terminals of ground/satellite communication systems. Of the two low-cost packaging concepts considered, the ball-grid-array concept was found to be worthy of further development and to offer the potential for cost-effective packaging of converter MMICs.

This work was done by Paul Blount of Hittite Microwave Corp. for **Glenn Research Center**. *Further information is contained in a TSP [see page 1].*

Inquiries concerning rights for the commercial use of this invention should be addressed to NASA Glenn Research Center, Commercial Technology Office, Attn: Steve Fedor, Mail Stop 4–8, 21000 Brookpark Road, Cleveland, Ohio 44135. Refer to LEW-16752.

Hardware, Techniques, and Processes

BLANK PAGE

Redundant Fiber-Optic Transceivers for Remote Testing

Data can be transmitted at rates up to 125 Mb/s over long distances.

Stennis Space Center, Mississippi

Redundant fiber-optic transceivers have been incorporated into the High Speed Data Acquisition System (HSDAS) at Stennis Space Center, where they are used to communicate data acquired by remotely located instrumentation during tests of spacecraft engines. These and similar transceivers could also prove useful in other situations in which there are requirements for acquiring data at safe distances from instrumentation located in hostile or potentially dangerous environments.

A primary consideration in the design of these transceivers is to separate the analog-to-digital conversion hardware from the data recording device. The analog signals from a test stand could be transmitted to a safe location over long copper cables, but the signals on the cables can become corrupted through pickup of electromagnetic noise from the environment. Another approach would be to avoid long cables by tape-recording the analog signals on the test stand and subsequently transporting the tapes to a safe location for processing. This method would require extra time to digitize the data after tests. Analog-to-digital conversion on the test stand, digital transmission, and recording at a remote location make it possible to avoid both the degradation of analog electrical signals over long cables and the delays incurred through post-test digitization.

With these transceivers, the analog instrumentation outputs are digitized and preprocessed on the test stand and then recorded remotely on a commercially available high-speed data recorder. Previously, the digitizer was connected to the recorder through a 75-Ω coaxial cable that could be no longer than 50 m. The electrical output of the recorder — a modified TAXI (Transparent Asynchronous Transmit/Receive Interface) signal containing a stream of digital data at a rate of 125 Mb/s — is fed through a standard duplex coaxial interface to the first of two fiber-optic transceivers. In the first transceiver, the electrical signal is converted to an optical one, then transmitted over one of two duplex fiber-optic links to the second transceiver, which is in a safe location far from the test stand. The fiber-optic link can be as long as 25 km — much longer than the coaxial cable. In the second transceiver, the optical signal is converted back to the original electrical signal and this data is then stored on the high-speed data recorder.

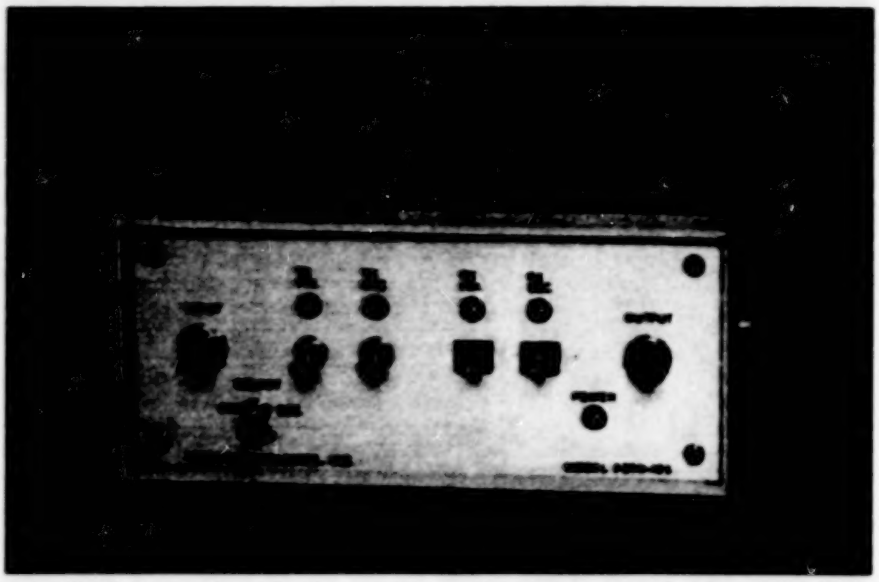

Fiber-Optic Transceivers like this one are used in pairs to transmit digital signals from remote test locations at rates up to 125 Mb/s. Whereas the maximum usable length of a coaxial cable for transmission of analog signals in the original application is 50 m, the maximum length of a fiber-optic digital link in the same application is 25 km.

Each transceiver (see figure) contains two fiber-optic transmitters and two fiber-optic receivers. Under either manual or automatic control, electronic switching circuitry in the transceivers selects the transmitter/receiver pair that generates the best received signal. The redundancy of transmitters and receivers also helps to prevent communication errors that could arise from defects in the fiber-optic links.

This work was done by Joey V. Kirkpatrick of **Stennis Space Center** *and Francis Grosz, Jr., Kenny Lannes, and David Maniscalco of Omni Technologies, Inc.*

This invention is owned by NASA, and a patent application has been filed. Omni Technologies, Inc., has an exclusive license for this technology. All inquiries should to addressed to: Omni Technologies, Inc., Attn: Sean Griffin, 7412 Lake Shore Drive, New Orleans, LA 70124, Tel No: (504)288-8211. Refer to SSC-00052.

Integrated Environmental Monitoring System for Clean Rooms

A system of electronic monitoring equipment under central computer control records and displays the readouts of environmental-quality instrumentation in clean rooms in the Space Station Processing Facility at Kennedy Space Center. The instruments include airborne-particle counters, temperature, humidity and pressure sensors, and detectors of ammonia and other gases. The monitoring system is readily configurable and expandable; it was developed to replace a system that was based on obsolescent computers and could not accommodate new instruments. The system includes a central data station, assembled from commercial hardware, that receives and records data, provides local and remote graphical user interfaces, provides security features, and prints reports. The central data station is connected to monitoring locations via RS-422 standard electronic communication links. At the monitoring locations, modular converters are used to convert between the RS-422 format and other digital or analog data

formats, which include the RS-232 and 0-to-5-volt formats. This is done in order to accommodate instruments that output data in these formats.

This work was done by Paul A. Mogan of Kennedy Space Center *and William L. Gill formerly of McDonnell Douglas Space Station Co. Further information is contained in a TSP [see page 1].*

Inquiries concerning rights for the commercial use of this invention should be addressed to the Technology Programs and Commercialization Office, Kennedy Space Center, (407) 867-6373. Refer to KSC-12044.

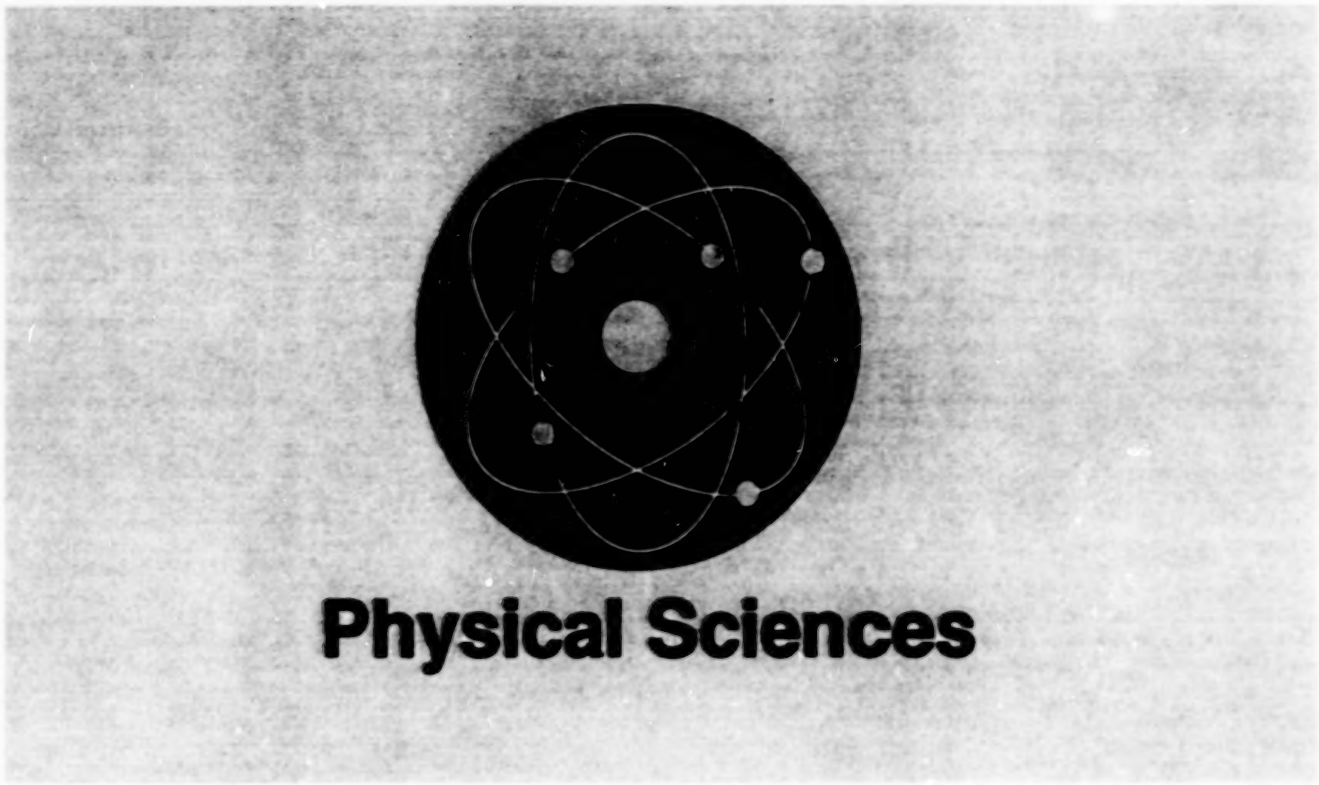

Physical Sciences

Hardware, Techniques, and Processes

BLANK PAGE

Camera Images Hydrogen Fires in Three Wavelength Bands

The camera filters and processing can be customized for other multispectral imaging applications.

Stennis Space Center, Mississippi

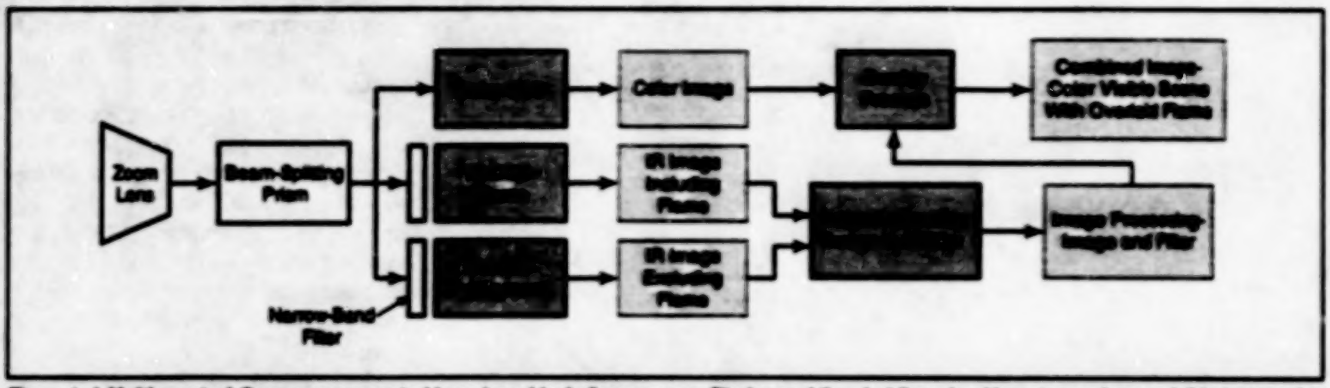

Figure 1. A Multispectral Camera represented here by a block diagram uses filtering and thresholding algorithms to produce a visible image of a typically transparent hydrogen fire.

A special-purpose multispectral video camera has been designed to provide an enhanced capability for viewing hydrogen fires. Hydrogen fires do not emit sufficient visible light to be seen by the unaided human eye, but they do emit strongly at other wavelengths — especially in the infrared and near-infrared portions of the spectrum. Therefore, like some other video cameras developed previously for the same purpose, this camera is designed to respond to infrared light emitted by hot water molecules in hydrogen flames. Going beyond previous designs, this camera provides a combination of imaging in three wavelength bands and processing of the three images, all for the purposes of (1) reducing spurious responses to background light and solar radiation and (2) synthesizing an image of a hydrogen flame overlaid on an ordinary visible-light image of the scene that contains the flame.

The camera includes custom optics similar to the color-separation prisms found in broadcast video cameras, but operating in different spectral regions. Instead of separating the red-green-blue light, this camera separates the incoming light into visible and two infrared channels. The incoming light is first focused by a commercial electronic news gathering (ENG) motorized zoom lens assembly, then passed through the prism to separate it into three spectral images.

The operation of the camera is illustrated in Figure 1. Incoming light passes through the zoom lens and beam-splitting prism. The visible wavelengths are routed to the color charge-coupled device (CCD) to acquire a standard color video image. The near infrared light is split into two different channels, one to image wavelengths corresponding to the flame emissions and another to image a near-infrared wave band that omits the flame emissions. The spectral content of the light arriving at the CCD sensors is selected by narrow-band filters placed in front of the imaging arrays.

The light arriving at the CCD array sensors is transformed into electronic image data. The outputs of the CCDs are digitized and processed using proprietary algorithms programmed into an Altera programmable logic device. The background infrared (IR) image is subtracted from the flame IR image. Filtering and thresholding algorithms isolate the flame pixels. The resultant isolated flame image is superimposed on the visible image producing a red overlay on the visible image, denoting the location and size of the hydrogen flames. A digital-to-video encoder provides a standard NTSC (National Television Systems Committee) and S-video output. Multiple modes provide output of the color, flame IR, background IR, or overlay image. Figure 2 shows the overlay mode image with the flame represented in red. The inset shows a standard color video image for comparison. An additional output mode cycles among color, flame IR, and overlay images at a fixed interval. User control of the output mode is available via remote-control input or a switch on the rear of the camera.

With an eye towards other types of future application, the camera was designed with a number of features to accommodate customized filtering and image processing. Alignment features built into each array channel allow image registration of the three images to less than one pixel accuracy. This allows the camera to be easily realigned after disassembly for filter replacement. The camera optical mounts are fabricated from low-expansion alloys to minimize temperature sensitivity. The onboard image processing is implemented with a programmable logic device that can be customized for special applications. Future versions of the camera will provide digital output from the three CCD arrays to provide a direct interface to computer systems for additional image processing.

Figure 2. The Processed Image of a Hydrogen Flame is superimposed in red against the background, making it clearly visible, whereas the standard color video image of the same scene in the inset does not reveal the flame.

This work was done by David B. Duncan, Greg Leeson, and Sherwood Kantor of Duncan Technologies, Inc., for **Stennis Space Center.**

In accordance with Public Law 96-517, the contractor has elected to retain title to this invention. Inquiries concerning rights for its commercial use should be addressed to

David B. Duncan
Duncan Technologies, Inc.
11824 Kemper Road
Auburn, CA 95603

Refer to SSC-00056, volume and number of this NASA Tech Briefs *issue, and the page number.*

Rapid Thermal-Cycle Life Testing of Thin Films

The thermal-cycle time is only 20 seconds.

Goddard Space Flight Center, Greenbelt, Maryland

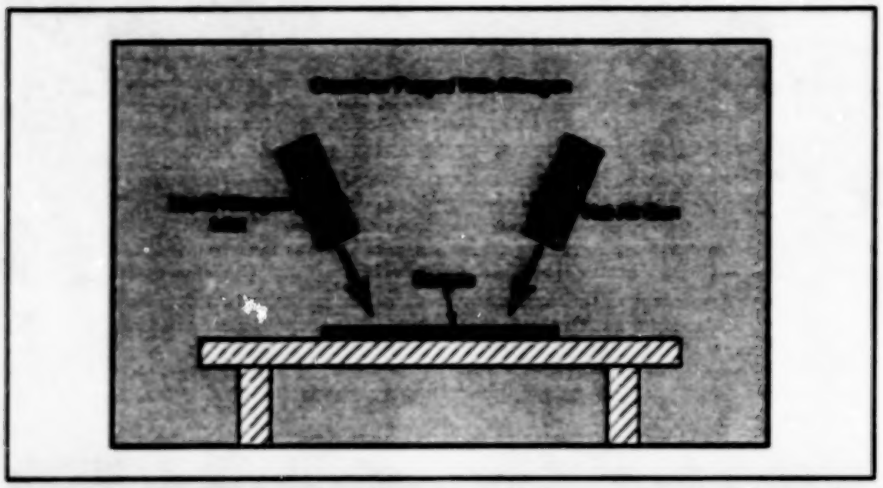

Samples Are Alternately Cooled and Heated by liquid nitrogen and electrically heated nitrogen, respectively, under automatic timing control.

An automated heating/cooling laboratory apparatus enables the accelerated thermal-cycle life testing of thin-film samples and other small material samples. In the original application for which the apparatus was constructed, the thin-film samples are candidates for use as components of thermal-insulation blankets, and there is a requirement to subject the samples to at least 20,000 thermal cycles between the temperatures of +50 and −100 °C. Without the present apparatus, it would be necessary to test the samples in an environmental chamber that takes about 30 minutes to complete a thermal cycle and would therefore take more than a year to complete 20,000 cycles. In contrast, the present apparatus operates with a thermal-cycle time of 15 to 20 seconds, making it possible to complete the 20,000 cycles in less than five days.

The apparatus includes a hot-air gun and a liquid-nitrogen inlet mounted above and aimed at the samples. All of the aforementioned components are located in a chamber purged with nitrogen (see figure). A solid-state relay is used to control the opening and closing of an electrically actuated valve that controls the flow of liquid nitrogen through the inlet. Another solid-state relay is used to turn the hot-air gun on and off. (Because the gun is located in the nitrogen-purged chamber, it actually blows hot nitrogen, not hot air, when it is turned on.) The samples are taped and clamped to a fixture. Thermocouples are attached to the fixture and to one of the samples for monitoring test temperatures.

The solid-state relays are toggled by an amplified 1-volt rectangular-wave signal that establishes the timing of the cooling and heating periods of the thermal cycle. When the signal is 1 V, the liquid-nitrogen valve is opened and the hot-air gun is turned off. When the signal is 0 V, the liquid-nitrogen valve is closed and the hot-air gun is turned on. The duty cycle of the rectangular wave is adjusted to obtain the required thermal cycle; for example, in initial experiments, the liquid-nitrogen valve was opened during about 38 percent of the thermal cycle and the hot-air gun was on during the remaining 62 percent of the cycle.

This work was done by Charles Powers and Bruno Munoz of **Goddard Space Flight Center.** *Further information is contained in a TSP [see page 1].*
GSC-13974

Determining Superconductor Inhomogeneity at Room Temperature

Eddy-current scans reveal inhomogeneities of resistivity, which is related to TC.

Marshall Space Flight Center, Alabama

A technique for determining inhomogeneities in a specimen of a high-critical-temperature superconductor involves scanning a small eddy-current probe over a flat surface of the specimen at room temperature while monitoring the inductance of the probe. In contrast, older techniques for obtaining the same or similar information involve cooling the specimen below its superconducting-transition critical temperature (T_C), with attendant difficulty and cost of operating a cryogenic apparatus.

The present technique is based on the following two concepts:

1. The inductance of a test coil placed near a highly electrically conductive object increases with increasing electrical resistivity of the object.
2. Previous measurements on conventional low-T_C superconductors have revealed correlations between their T_Cs and normal resistivity ratios. High-T_C superconductors are assumed to behave similarly.

Applying these concepts to a specimen of a high-T_C superconductor, one can infer inhomogeneities (specifically, spatial variations of T_C, including intergrain contacts and structural defects) from spatial variations of room-temperature resistivity and thus from spatial variations of the inductance of an eddy-current probe scanned over the specimen.

Figure 1 schematically depicts an apparatus for implementing the technique. An eddy-current probe is held stationary just above the flat surface of a high-T_C specimen, which is mounted on a horizontal two-dimensional (x,y)-translation table. Stepping motors controlled by a computer actuate the translation stages to move the specimen to commanded x,y positions. By use of a variable-frequency inductance/capacitance/resistance meter, the coil is excited at a frequency (typically about 10 MHz) chosen to obtain the best signal-to-noise ratio and the inductance of the coil is measured. This measurement is repeated at regular increments (typically 0.5 mm) of x and y to obtain a map of eddy-current-probe inductance on a rectangular grid that

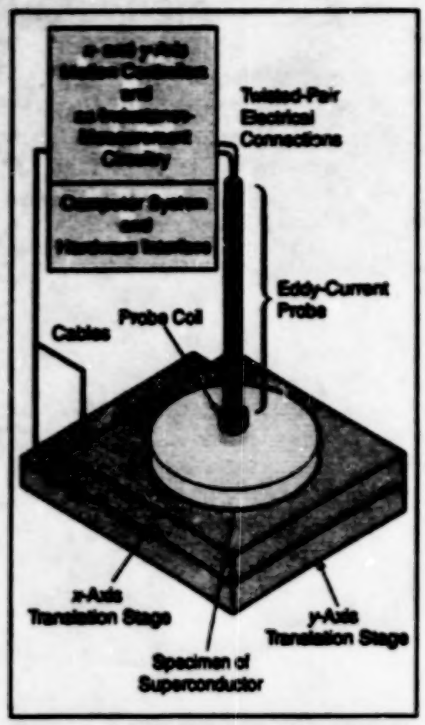

Figure 1. A Flat Specimen of a High-T_c Superconductor is translated under an eddy-current probe to obtain local probe-inductance measurements at the intersections of a rectangular grid.

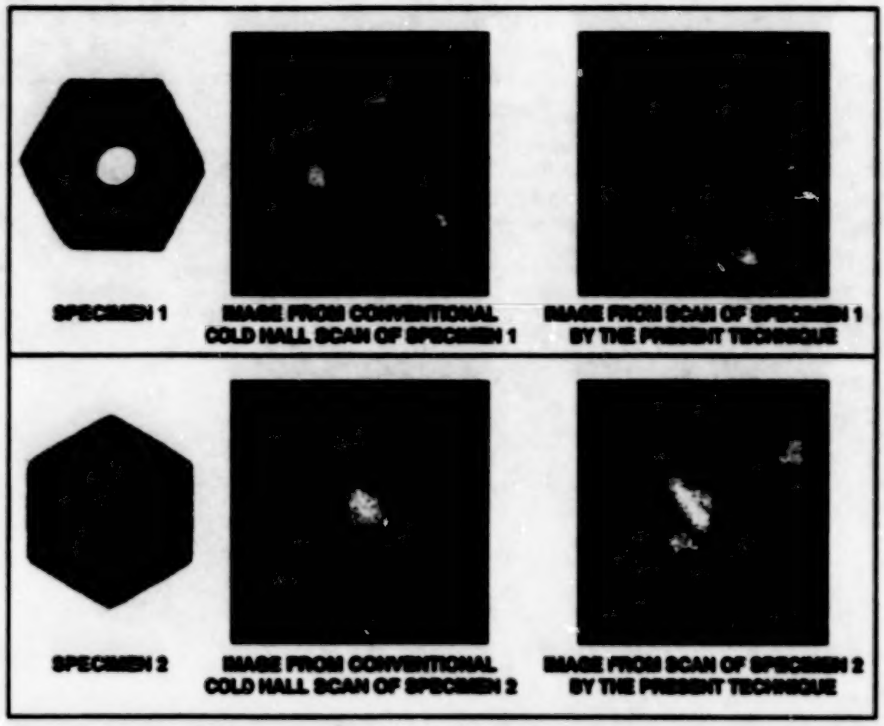

Figure 2. Images of Inhomogeneities in two high-T_c-superconductor specimens were synthesized from Hall-probe scans at low temperature and from room-temperature scans by the present technique. A qualitative correlation between the two images for each specimen is apparent.

spans the specimen surface. The inductance data at the grid points can be used to synthesize a gray-scale or false-color image of inhomogeneity in the specimen (see Figure 2).

This work was done by Robert C. Sisk and Palmer N. Peters of **Marshall Space Flight Center.** *Further information is contained in a TSP [see page 1].*

Inquiries concerning rights for the commercial use of this invention should be addressed to the Patent Counsel, Marshall Space Flight Center [see page 1]. Refer to MFS-31249.

Low-Current Cathodic Protection of Metal

The anode would be incorporated into a multilayer protective coat.

Langley Research Center, Hampton, Virginia

A proposed extension of the impressed-current method of cathodic protection of metal against corrosion in wet environments would reduce the current and power needed. The proposal involves (1) the application of a special multilayer coat to the metal part to be protected and (2) the use of a small dc power supply that operates at a precisely chosen low output potential. The effectiveness of protection should justify the costs of power sources and coatings in many situations: metal structures that could be protected by the extended method include ships, automobiles, bridges, metal buildings, radio towers, pipelines, and storage tanks.

The proposed multilayer protective coat would include an electrically insulating layer in contact with the metal surface to be protected. The next layer would be electrically conductive; it could be made of conductive plastic or carbon-filled paint, for example. If the conductive layer were not sufficiently durable to withstand prolonged exposure to the anticipated environment, a third protective layer could be added. The conductive layer would be connected to the positive terminal of the dc power supply, while the metal to be protected would be connected to the negative terminal (see figure).

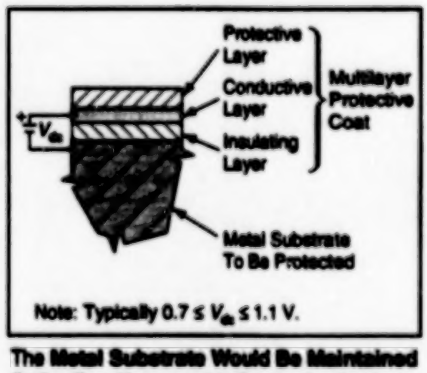

The Metal Substrate Would Be Maintained Cathodic with respect to the conductive layer in the protective coat.

If there were no cracks or pinholes in the multilayer coat, then when the power supply was first turned on, current would flow initially by virtue of the capacitance between the metal substrate and the conductive layer. Once the capacitor was charged to the output potential of the power supply, the current would fall to a negligible value, and only a static electric field would be maintained. As cracks or pinholes formed during deterioration of the outer layers, water and oxygen would come in contact with the metal substrate. By keeping the metal substrate negative (cathodic) relative to the conducting layer, a protective shield of hydrogen ions would be made to form on the exposed parts of the metal sub-

strate, thereby inhibiting electrochemical reactions in the pinholes and cracks.

To protect effectively against corrosion, in the presence of water, the output potential of the power supply must be greater than the corrosion-induced potential of the metal substrate. For example, the potential for iron to corrode to common rust is 0.44 V. At the same time, the supply voltage should be less than the minimum voltage to electrolyze water (1.229 V), so that the impressed current could be kept much smaller than it would be if electrolysis were occurring. On the basis of previous experience with sacrificial anodes of zinc (which has an oxidation potential of 0.76 V), it appears that a suitable potential to protect steel without consuming excessive current in electrolysis would lie between 0.7 and 1.1 V.

This work was done by Leonard M. Weinstein of Langley Research Center. *LAR-15069*

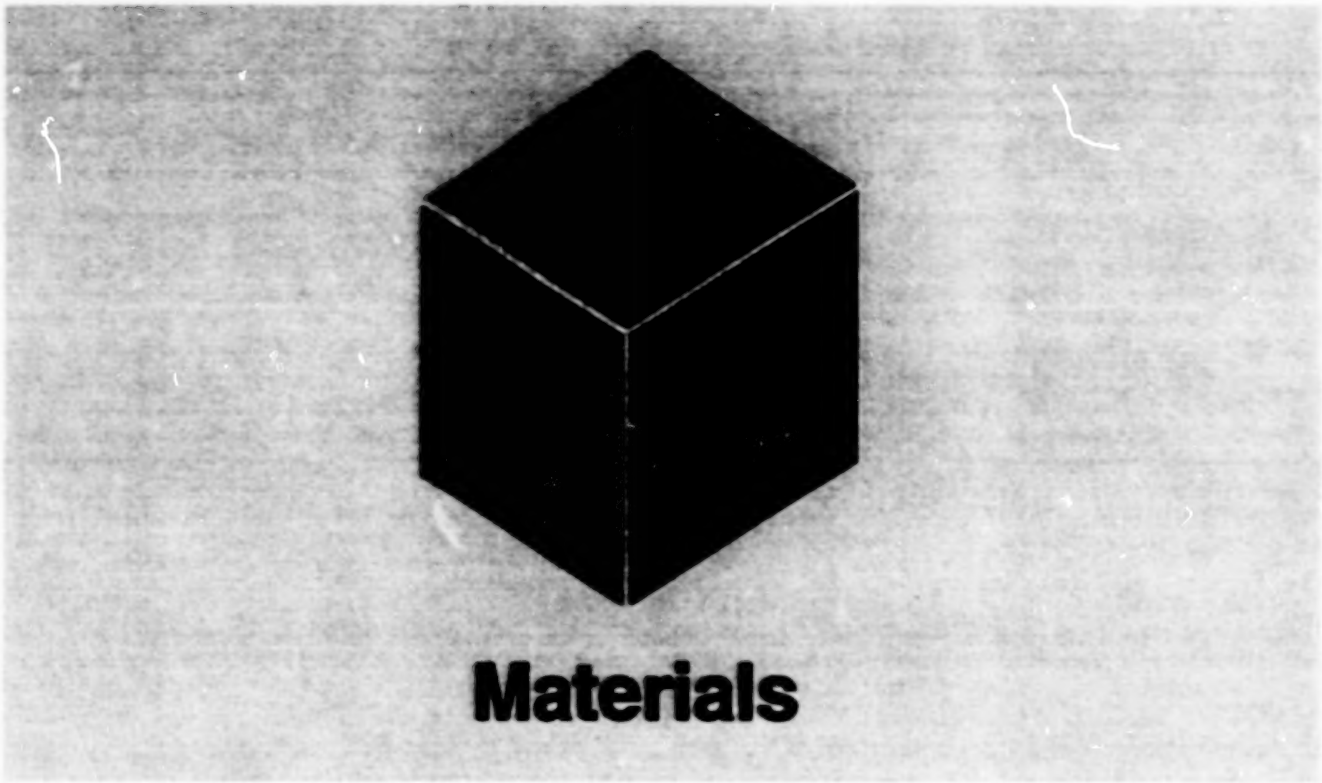

Materials

Hardware, Techniques, and Processes

BLANK PAGE

Fabricating Diamond Membranes Using Reactive-Ion Etching

The rate of dry etching of silicon is more than 3 times that of hot KOH.

NASA's Jet Propulsion Laboratory, Pasadena, California

A process for the fabrication of a polycrystalline diamond membrane involves chemical vapor deposition (CVD) of diamond onto a silicon substrate, followed by conventional photolithography and subsequent reactive-ion etching to remove part of the substrate (see figure). This process is an improvement over an older process in which the substrate is etched in a hot KOH solution. This process can be used to fabricate diamond polycrystalline membranes as parts of microelectromechanical sensors.

The starting substrate is a mirror-smooth (100)-oriented single-crystal silicon wafer with n or p doping to a resistivity <20 Ω-cm. To increase the density of nucleation sites for diamond and thereby make it possible to obtain a pinhole-free diamond deposit, the front (top in the figure) surface of the substrate is scratched by use of diamond paste. A polycrystalline diamond film is grown on the scratched surface by CVD from a flowing mixture of methane and hydrogen, typically at a total pressure of 45 torr (6 kPa) and a substrate temperature of 950 °C.

After deposition of diamond to the required thickness, aluminum is deposited on the back (bottom in the figure) surface of the substrate by electron-beam evaporation. The aluminum film is patterned photolithographically, then etched by a commercial solution containing phosphoric and acetic acids, thereby forming a mask to define the areas to be protected from, and exposed to, reactive ion etching. Next, reactive-ion etching is effected by use of a radio-frequency-induced SF_6 plasma.

In an experiment, the rate of reactive-ion etching was found to be about 3.6 μm per minute; in contrast, the rate of etching in hot KOH is about 1 μm per minute. It was also found that reactive-ion etching undercut the masked portion of the substrate at a rate of about 3.5 μm per minute. The diamond membrane exposed by etching of the substrate was found to be in a state of compressive stress.

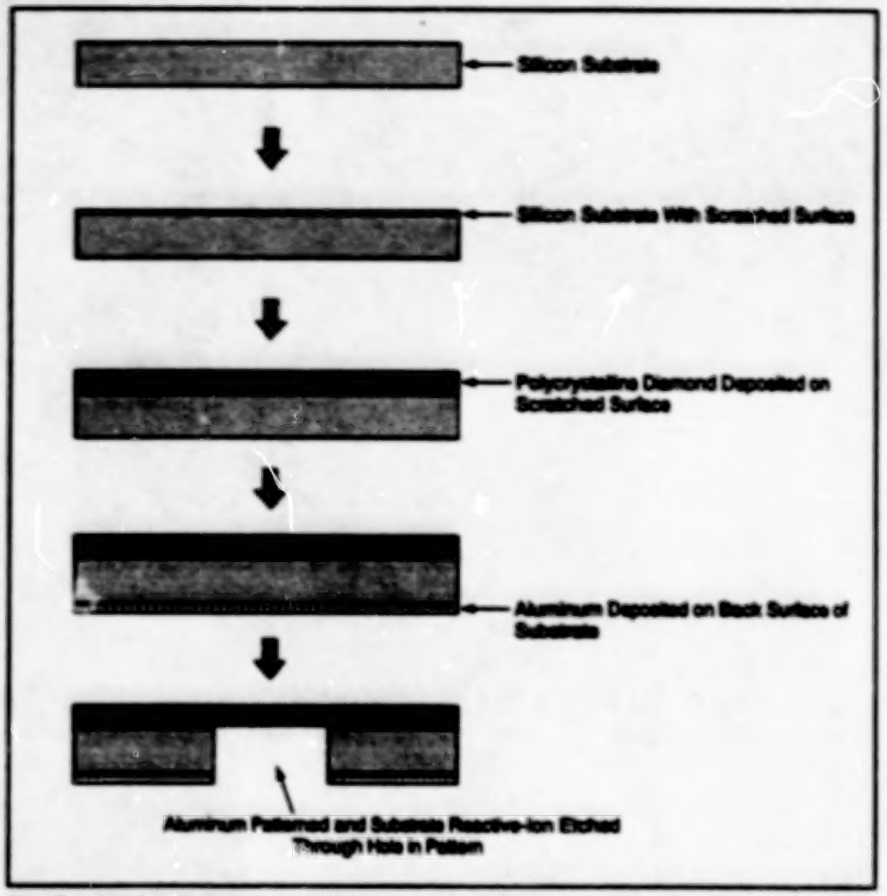

The Processing Sequence is depicted here schematically in terms of the status of the workpiece at various stages.

This work was done by Rajeshuni Ramesham of Caltech for NASA's Jet Propulsion Laboratory. Further information is contained in a TSP [see page 1].

NPO-20477

Metal-Surfaced Ceramic Insulating Blankets

Metal foils are attached to ceramic blankets by brazing at multiple locations.

Ames Research Center, Moffett Field, California

Flexible thermal-insulation blankets made of ceramic fibers can be protected against weather and handling by attaching thin metal face sheets. In applications in which the blankets are exposed to gas flows, the face sheets also afford protection against flow-induced stresses and help reduce aerodynamic drag by providing smoother flow surfaces.

Typically, a metal sheet to be attached to a ceramic blanket has a thickness of 5 mils (~0.13 mm) or less and is made of titanium, aluminum, chromium, niobium, or alloys of these elements. The blanket can be made of fibers of silica, aluminoborosilicate, silicon carbide, and/or other ceramic materials. Optionally, in preparation for attachment of the metal sheet, the ceramic fabric on the attachment surface of the blanket can be precoated with a thin layer of nickel to improve its bonding properties.

Small dots of a metal or ceramic brazing material are placed on the attachment surface of the blanket (see figure). Preferably, the dots are between 1/8 and 1/4 in. (about 3 to 6 mm) square and positioned either randomly or in a regular pattern at intervals of about 1 in. (~2.5 cm). The metal or ceramic brazing material can be any of several commercial formulations that both wet the ceramic fabric and form metallic bonds with the metal sheet when heated to the brazing temperature.

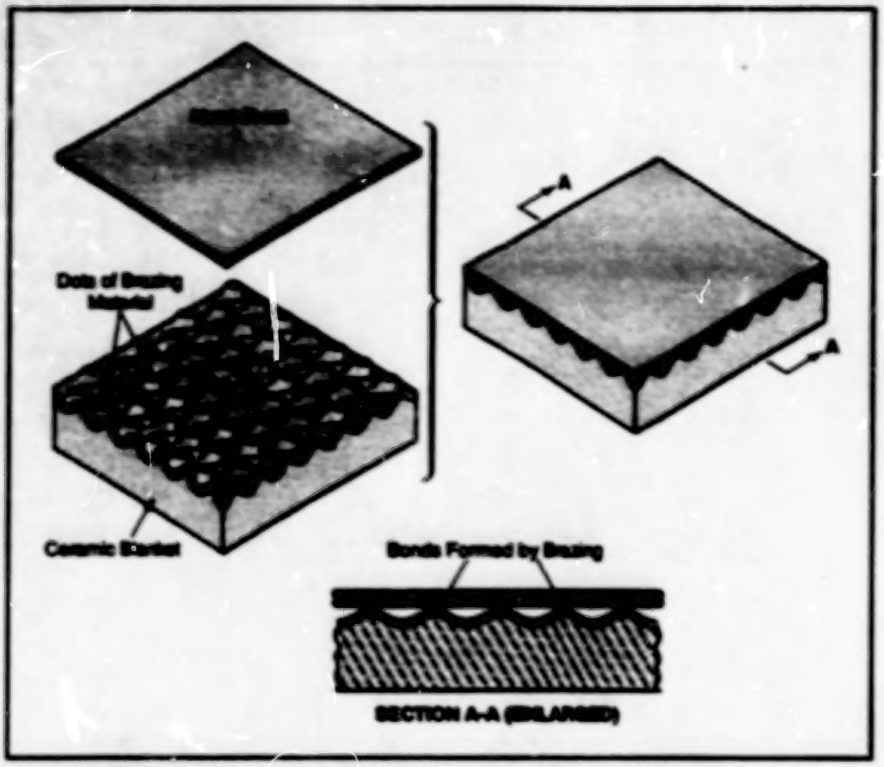

The Metal Sheet and the Ceramic Blanket are joined by brazing at the dots.

Suitable ceramic brazing materials include ceramic-precursor adhesives based on silica, alumina, and/or zirconia. Suitable metal brazing materials include copper/silver, copper/gold, and copper/silver/gold alloys that contain titanium and/or vanadium as wetting agents.

The metal sheet is placed over the dots, then the resulting sandwich is heated to a temperature of about 1,800 °F (about 980 °C) in a reducing atmosphere or in a vacuum to effect brazing. Finally, the sandwich is cooled to room temperature, leaving the metal sheet strongly bonded to the blanket at the dots.

This work was done by Daniel J. Rasky, Paul M. Szawlo, Paul Kolodziej, and Demetrius A. Kourtides of **Ames Research Center**. *Further information is contained in a TSP [see page 1].*

This invention has been patented by NASA (U.S. Patent No. 5,744,252). Inquiries concerning nonexclusive or exclusive license for its commercial development should be addressed to the Patent Counsel, Ames Research Center [see page 1]. Refer to ARC-11989.

Separating Ethanol From Water Via Differential Solubility

Alcohol for combustion could be purified more economically.

Langley Research Center, Hampton, Virginia

The differential solubility of sulfur in ethanol and water could be exploited to separate ethanol from water. The energy that could be produced by burning the separated ethanol would be more than that required in the separation process. In contrast, the separation of a small amount of ethanol (actually an ethanol/water solution poor in ethanol) from water by distillation requires more energy than can be produced by burning the resulting distillate. The proposed alcohol/water separation process could be exploited industrially to produce clean fuel from fermented vegetable matter.

In one version of this concept, sulfur would be added to an ethanol/water mixture; a slight amount of sulfur that depends on the temperature of the mixture would be dissolved by the ethanol. (All three forms of sulfur are insoluble in water, even at its boiling temperature, but the α form of sulfur is slightly soluble in ethanol and the β form is more soluble in ethanol, according to the *CRC Handbook of Chemistry and Physics*.) The sulfur/ethanol mixture would settle to the bottom of the container, where it could be bled off. This small part of the original mixture could then be heated to separate the volatile ethanol from the significantly less volatile sulfur. The hot sulfur left after the distillation could be added to another batch of the ethanol/water mixture.

In comparison with the energy consumed in the conventional distillation process, a significant amount of energy would be saved in this process because only the small bled-off portion of the original mixture would have to be heated. Because of its solubility in ethanol, the β form of sulfur would be used when the separation process was carried out at room temperature and atmospheric pressure. Finely divided sulfur that was not dissolved by the ethanol would float on the mixture.

In an alternative version of this concept, the ethanol/water/sulfur mixture would be placed in a retort, where it could be heated and pressurized to a temperature above the critical temperature and pressure of ethanol [243 °C and 63 atm (6.4 MPa), respectively] but below the critical temperature and pressure of water [374.1 °C and 218.3 atm (22.12 MPa), respectively]. The mixture would be retorted at a temperature slightly above 243 °C and at a pressure slightly above 63 atm (6.4 MPa), putting the ethanol in the supercritical state, in which it should easily dissolve all three forms of sulfur (including the γ form, which is insoluble at ambient temperature and pressure). The water, on the other hand, would still be well below its critical state and still should not dissolve sulfur. The sulfur/ethanol mixture would settle to the bottom of the retort, where it could be piped away under pressure and at high temperature. The sulfur/ethanol mixture would then be expanded to a lower temperature and pressure at which not as much sulfur could be dissolved in the ethanol and at which ethanol would partially separate from the mixture. Further heating of the remaining mixture at a pressure of 1 atm (0.1 MPa) would separate most of the remaining ethanol and sulfur. The sulfur could be reused, and the high-pressure hot water could be used to cook more mash to be fermented or to preheat a charge going to another retort.

This second version is probably the most suitable for an industrial process, and could be aided by the addition of a centrifuge to separate the initial two-phase mixture. The role of sulfur in both versions could be played by another substance. However, the low toxicity and very low vapor pressure of sulfur at the boiling temperature of ethanol appear to make it the best candidate.

This work was done by Renaldo V. Jenkins of **Langley Research Center**. *LAR-14894*

Separating Ethanol From Water Via Differential Miscibility

Alcohol for combustion could be purified more economically.

Langley Research Center, Hampton, Virginia

The differential miscibility of castor oil in ethanol and water would be exploited to separate ethanol from water, according to a proposal. Burning the separated ethanol would produce more energy than would be consumed in the separation process. In contrast, the separation of a small amount of ethanol (actually an ethanol/water solution poor in ethanol) from water by the conventional process of distillation requires more energy than can be produced by burning the resulting distillate. As in the process described in the preceding article, "Separating Ethanol From Water Via Differential Solubility" (LAR-14894), the proposed alcohol/water separation process could be exploited industrially to produce clean fuel from fermented vegetable matter.

In one version of this process, castor oil would be added to an ethanol/water solution. The ethanol would mix freely with castor oil, which is insoluble in water. The resulting ethanol/castor-oil phase, which would contain less than 1 percent water, would collect as the top layer, the bottom layer being the remainder of the ethanol/water solution somewhat depleted in ethanol. Heating this two-layer mixture to a temperature slightly below the boiling temperature of ethanol (78.5 °C) would cause the partial pressure of ethanol above the top layer to be much greater than the partial pressure of either castor oil or water. This vapor-phase ethanol could be condensed in a relatively pure state.

Although heating an isolated ethanol/water solution like that in the bottom layer would normally raise the vapor pressure of both ethanol and water above the solution, this would not be the case in the presence of the top castor-oil/ethanol layer for the following reasons: The amount of water that could dissolve in the top castor-oil/ethanol layer would increase only slightly upon heating. On the other hand, ethanol could readily cross the interface between the two layers and enter the top layer. As long as the total mix was kept at a temperature below the boiling temperature of ethanol (thereby preventing agitation of the layers by boiling), the diffusion of water through the castor-oil/ethanol phase would be inhibited.

In an alternative version of this concept, the upper castor-oil/ethanol layer would be skimmed off and heated to obtain the ethanol. Once the ethanol was driven off, the castor oil could be returned to an ethanol/water solution to dissolve more ethanol to repeat the process. This concept could readily lend itself to a continuous process. Substances other than castor oil (one of its components perhaps, or another substance) could be used in this process or to extract other compounds from other mixtures by using this upper-of-two-phases vaporization technique.

This work was done by Renaldo V. Jenkins of **Langley Research Center**.
LAR-14895

BLANK PAGE

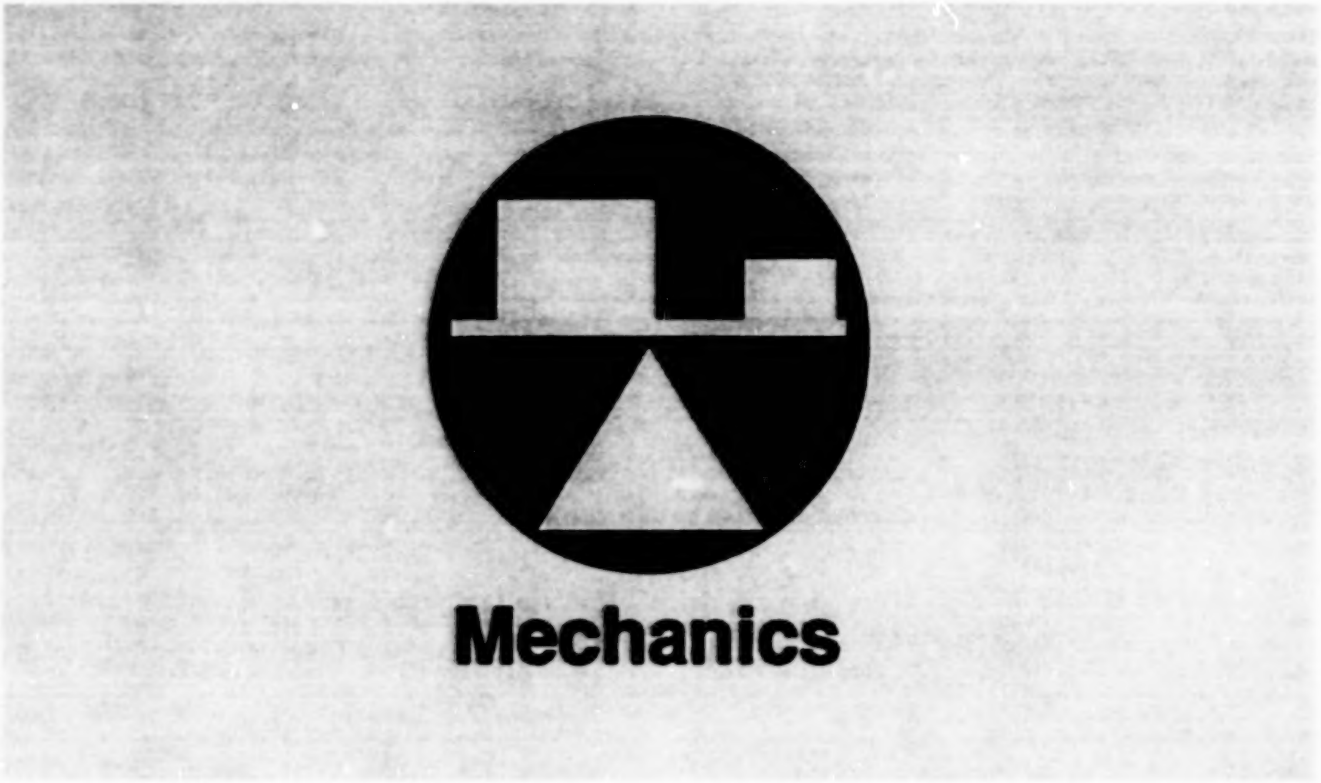

Hardware, Techniques, and Processes

BLANK PAGE

Durability Studies on the F-15B Flight-Test Fixture

X-33 and space-shuttle insulation specimens were tested by use of similar hardware.

Dryden Flight Research Center, Edwards, California

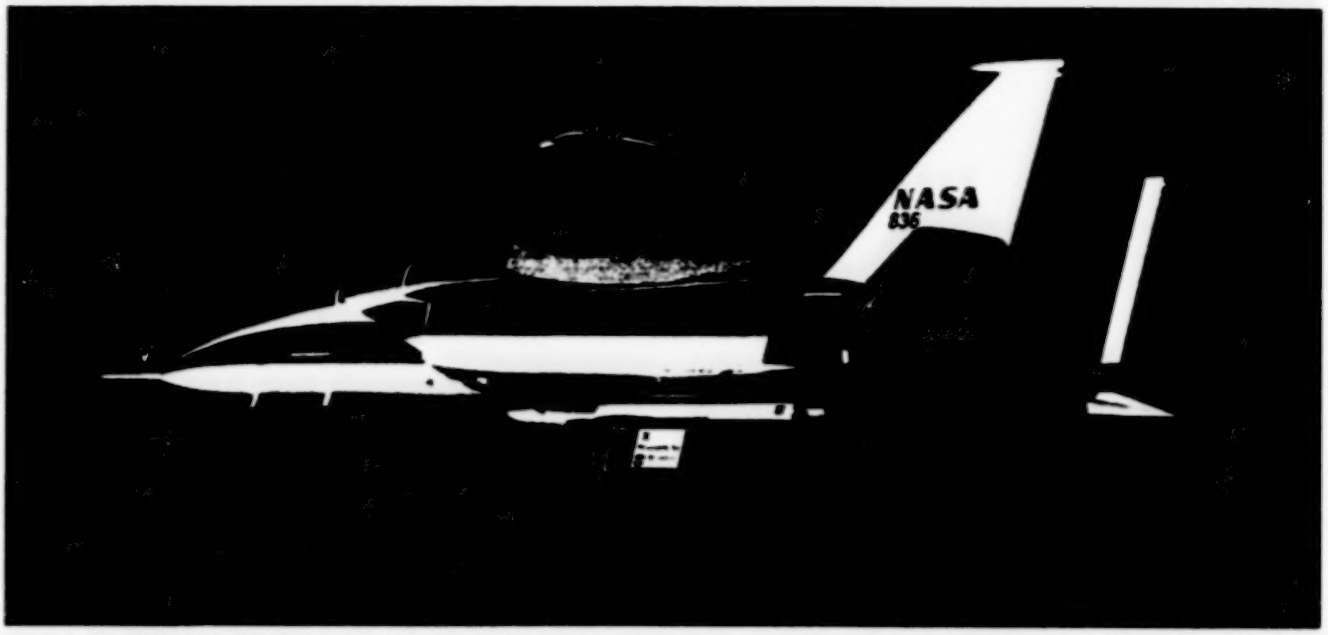

Figure 1. The **Flight-Test Fixture** is a fully instrumented test article mounted on the centerline of the lower fuselage of an F-15B airplane. The fixture is 107 in. (2.72 m) long, 32 in. (0.81 m) high, and 8 in. (20 cm) wide, with a 12-in. (30.5-cm) elliptical nose section.

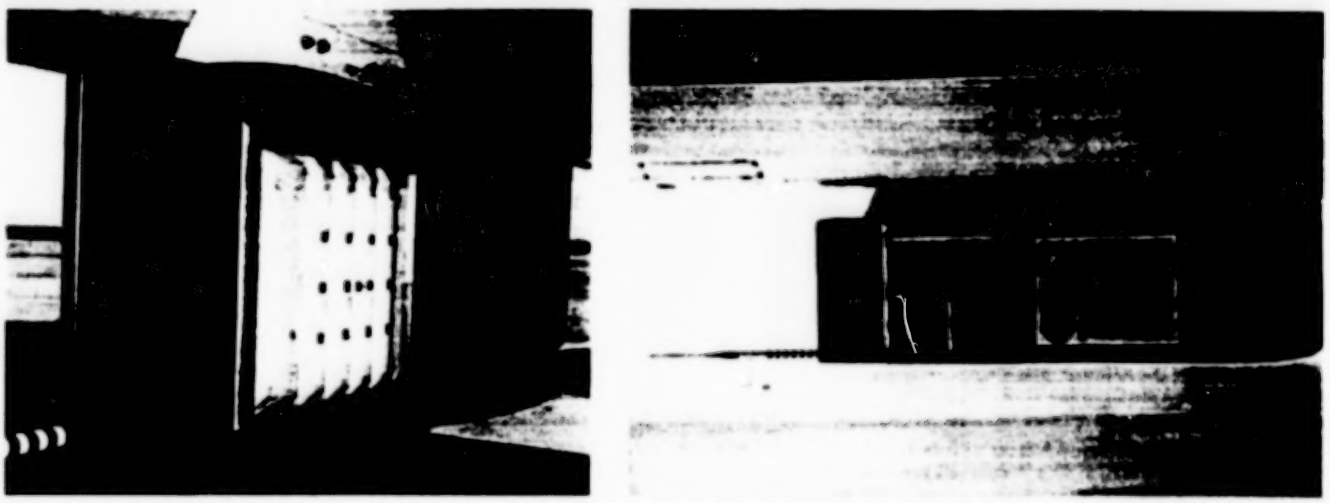

Figure 2. **Specimens of Exposed Materials** from the X-33 launch vehicle and the external tank of the space shuttle were mounted on the carrier plate of the flight-test fixture.

NASA's F-15B #836 is a two-seat version of the F-15, which is a high-performance, supersonic, all-weather fighter airplane. The F-15B is used as a test-bed aircraft for a wide variety of flight experiments. In support of this use, a flight-test fixture (FTF; see Figure 1) was developed to provide a space for flight experiments in a region with known aerodynamic conditions.

The FTF has been flown in many flight experiments during the past several years and can be modified to satisfy a variety of research requirements. For example, the X-33 project requested assistance in exposing specimens to shear and impinging shock loads for validation and flight qualification of the X-33 thermal protection system (TPS) materials in a flight environment. X-33 TPS materials for this experiment ranged from metallic panel materials (supplied by BF Goodrich) to a variety of advanced flexible reusable surface insulation (AFRSI) specimens supplied by NASA Ames Research Center. Traction seals and flight-test instrumentation gauges were also incorporated into the specimens to demonstrate the durability of these components. Some of the specimens were thermally cycled in an arc-jet tunnel prior to flight test in order to simulate thermal loads expected on the X-33 vehicle.

The two forward left side panels on the FTF were replaced by a large carrier plate in order to simplify the installation of the various TPS specimens and thereby enable quick changes in configuration between research flights. Specimens were installed in the various quadrants of the carrier plate (see upper part of Figure 2), depending on the desired configuration for each flight. Forward specimens were generally used to look at the effects of shock-

impingement loads previously identified at forward locations at transonic speeds. Specimens in the aft locations were used to document the effects of shear loads.

Six configurations were flight-tested at a maximum mach number of 1.4 and dynamic pressures as high as 790 lb/ft^2 (37.8 kPa). Flight tests were conducted at altitudes as low as 5,000 ft (1.5 km) to obtain the higher shear loads and as high as 35,000 ft (10.7 km) for supersonic testing. Surface pressures were obtained to document flow conditions and loads on the specimens. In addition, in-flight video and detailed pre- and post-flight photos were used to document the conditions of all specimens. This highly successful flight-test series was completed in May 1998 as part of the overall flight qualification of the X-33 TPS.

Several months later, the Shuttle External Tank Project from Marshall Space Flight Center saw the results of the X-33 test and requested use of the same carrier plate to expose specimens of the shuttle external tank insulation to a simulated shuttle launch environment at speeds up to mach 1.5 and altitudes up to 60,000 ft (18.3 km). Six specimens were flown to simulate the thrust-panel rib structure and foam where the shuttle solid rocket boosters are attached to external tank. Several types of foam insulation configurations and rib orientations (see lower part of Figure 2) were tested by use of similar instrumentation and video documentation. This flight-test series was successfully completed in less than two weeks in January 1999.

The X-33 and Shuttle External Tank Projects were both able to gain significant benefits from the flight-test results obtained by use of the F-15B FTF with a canter plate as a research platform. Flight results were obtained quickly and efficiently and provided valuable data toward flight qualification with an increased understanding of the durability of the tested materials in flight environments.

This work was done by David Richwine, Craig Stephens, Kirsten Carpenter, Michelle Gresilk, and David McAllister of **Dryden Flight Research Center**.
DRC-99-11

Suspension Devices for Vibration Testing of Structures

Springs, cables, and noncircular cams suspend objects in static equilibrium.

Langley Research Center, Hampton, Virginia

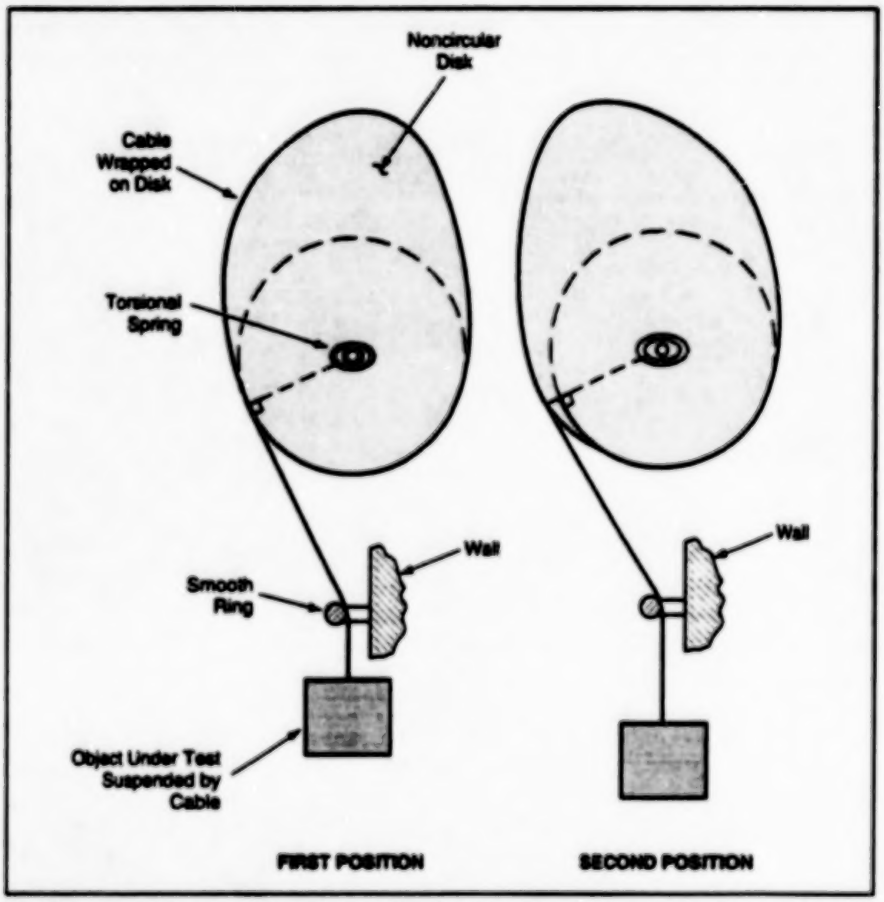

The Increase in Torque of the Torsional Spring when the object moves to the second position is balanced by an increase in the moment arm on the noncircular disk, keeping the object in static equilibrium at any height.

Space structures in general experience free-free vibrational boundary conditions that are not readily replicable on the ground. To conduct vibration tests of such structures on Earth, special devices must be used to support the weight of the structures without introducing any constraining forces that impose boundary conditions that detract from the simulation of the desired free-free boundary conditions in outer space. Previous supports all have certain disadvantages. For example, long cables entail very tall ceilings and generate undesirable pendulum effects, the masses of air pads incorporated into a suspended structure can distort the dynamical characteristics of the structure, pneumatic/electric devices are usually highly complex, and springs are limited by small domains of operation (strokes). To overcome these difficulties, a simple and inexpensive support was designed that includes a noncircular cam, a torsion spring, and a cable.

As shown in the figure, a thin cable is wrapped around the circumference of the noncircular disk. This cable passes through the smooth ring and extends downward to suspend the object under test. To prevent the cable from driving the disk and unwinding, a torsional spring is attached to the disk. The cam has a special profile designed in conjunction with the load it is to suspend and with the stiffness of the torsional spring. The torsional spring loads the cam as the cam rotates so that the torque exerted by the spring about the axis of rotation of the cam is exactly counterbalanced by the weight of the object under test.

In this concept, the profile of the disk is designed such that for any given displacement of the object under test from its original static-equilibrium position, its new position is also one of static equilibrium. This imitates what happens in

outer space: any object displaced from one position of static equilibrium to another position remains in static equilibrium in its new position.

This device also simulates the behavior of the object under test when it is subjected to an impulse. When a given velocity is imparted to the object, it continues to travel at that same velocity over a considerable range. The velocity remains constant because the tension in the cable remains constant and equal to the weight of the object, so that no net driving force is exerted on the article throughout its entire range of motion. This condition simulates the motion of an object in outer space.

This suspension system is simple and inexpensive to construct. The setup is very compact, precluding the need for high ceilings or large platforms. The range of motion for the object under test can be large, providing considerably longer times for the experimental collection of data. In addition, the inertia of the system is small and therefore does not appreciably modify the dynamical characteristics of the test article. Besides the obvious applications of this system in the aerospace field, it could be applied to many everyday problems in which objects must be balanced vertically by use of systems of relatively low mass and friction.

This work was done by Meng-Sang Chew and Li-Fam Yang of Old Dominion University, and Jer-Nan Juang of **Langley Research Center**. *Further information is contained in a TSP [see page 1].*

This invention has been patented by NASA (U.S. Patent No. 5,207,110). Inquiries concerning nonexclusive or exclusive license for its commercial development should be addressed to the Patent Counsel, Langley Research Center [see page 1]. Refer to LAR-14272.

BLANK PAGE

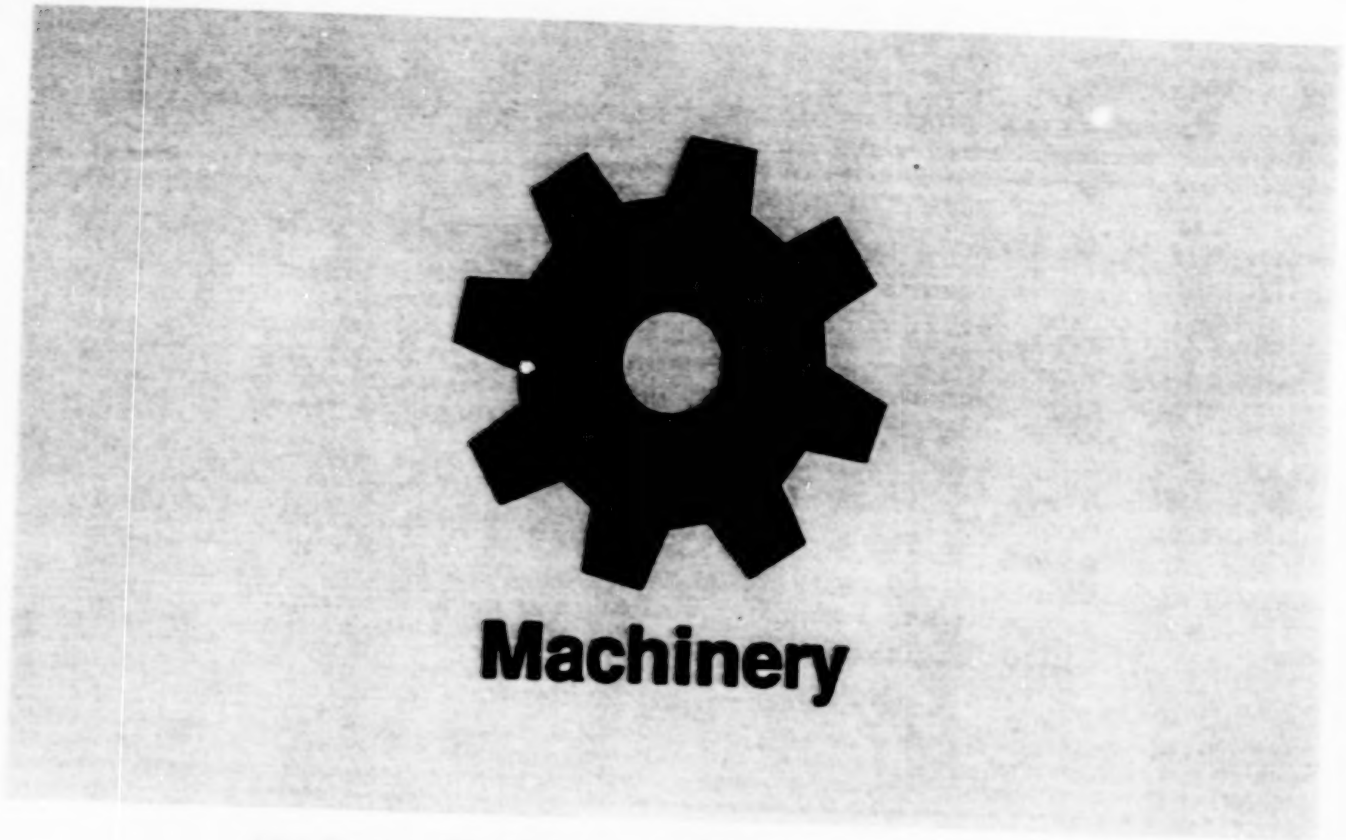

Machinery

Hardware, Techniques, and Processes

Books and Reports

BLANK PAGE

Pistol-Grip Torque-Measuring Power Tool

Features include compactness and improved control of torque.

Goddard Space Flight Center, Greenbelt, Maryland

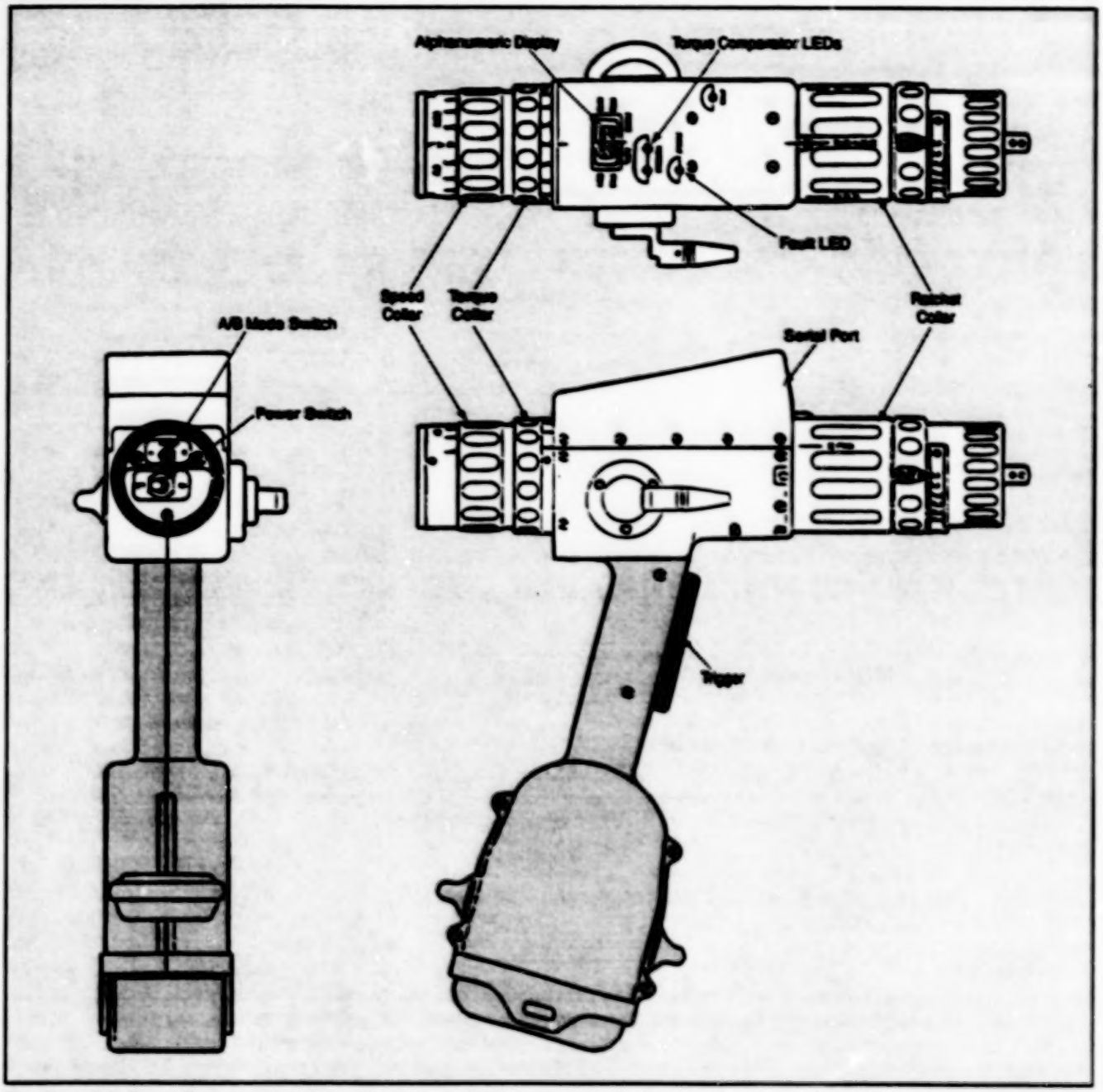

This Pistol-Grip Power Tool resembles other pistol-grip power tools in some respects, but is smaller and provides better control over applied torques.

The figure shows one aspect of the exterior appearance of a pistol-grip torque-measuring power tool. The tool is a self-contained, computer controlled, 3/8-in. (=9.5-mm) drive pistol-grip style tool. The tool is intended for use in assembly operations in which application of precise torques to fasteners is critical to safety. In comparison with controlled-torque industrial and commercial power tools now in use, the tool offers advantages of small volume and more precise control of torque. It can also be operated under battery power, with battery life extended relative to battery lives of similar commercial power tools.

The tool is capable of generating torques up to 25 lb-ft (34 N-m) and operating at speeds up to 60 revolutions/min. Numerous torque, speed, and turn count limits can be programmed into the tool through the tool's serial port. The tool is 14.17 long by 15.18 in. high (36.0 by 38.6 cm), with battery, and 2.75 in. (7.0 cm) wide.

Whereas currently available controlled-torque power tools feature open-loop servocontrol with poor torque-control accuracy, the tool includes a computer-based closed-loop servocontrol system that is programmed via software. The tool provides excellent torque-control accuracy. For each significant torque application event, the

tool records data in its nonvolatile memory. Each datum characterizes the maximum applied torque and angle rotated after a threshold torque is reached. The data may be downloaded to a separate computer to ascertain the quality of the torque application and to diagnose the condition of the tool.

This work was done by Paul W. Richards, Ken Wagner, Robyn King, and Chan Park of **Goddard Space Flight Center**; *Carl Konkel, Chris Smith, Joe Rood, and Leland VanAlen of Orbital Sciences Corp.; and Lee Brown, Randy Frey, and Mike Garrah of Swales. Further information is contained in a TSP [see page 1].*

This invention is owned by NASA, and a patent application has been filed. Inquiries concerning nonexclusive or exclusive license for its commercial development should be addressed to the Patent Counsel, Goddard Space Flight Center [see page 1]. Refer to GSC-13706.

Apparatus for Testing Vacuum Torsional Dampers

Variations in torque can be measured under realistic operating conditions.

Goddard Space Flight Center, Greenbelt, Maryland

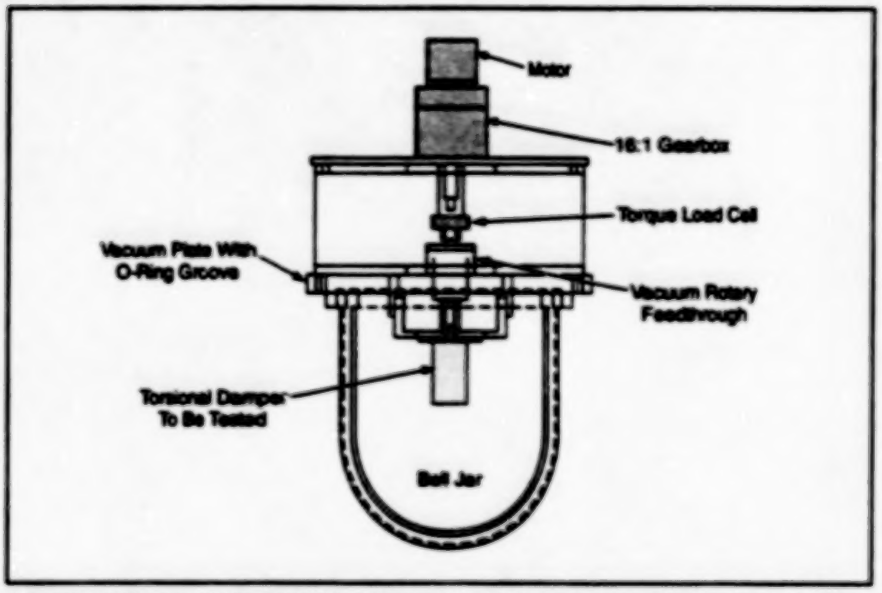

A Torsional Damper Is Actuated in a Vacuum while its responsive damping torque is measured by a load cell. Optionally, an x-ray camera (not shown) can be used to view bubbles in the liquid inside the damper.

A laboratory apparatus called a "vacuum damper investigation and performance evaluation robot" ("V-DIAPER") affords capabilities for vacuum dynamic testing of torsional dampers. The apparatus was developed for original use in testing torsional dampers (rotary viscous dampers) that are destined to operate, in vacuum, as parts of rotary solar-panel-deployment and antenna-deployment mechanisms on spacecraft. The V-DIAPER can also be used to perform vacuum dynamic testing of torsional dampers designed for terrestrial use in vacuum or in air.

In the original application, for which the V-DIAPER was developed, each damper contains a paddle that, in operation, is rotated through a highly viscous liquid in a chamber. By virtue of the rotation, the liquid is forced through an orifice from the advancing side to the retreating side of the paddle; this action contributes a major portion of the damping torque. The flow of the viscous liquid in the clearance between the paddle and the chamber walls also contributes some damping torque. When the damper is placed in a vacuum, bubbles can form in the damping liquid. The bubbles cause local decreases in viscosity and thus intermittent sharp decreases in damping torque during rotation. The V-DIAPER was designed to facilitate investigation of the effects of the bubbles under realistic vacuum operating conditions.

The V-DIAPER (see figure) includes a motor and gearbox for rotary actuation of a damper under test. The damper is mounted inside a vacuum bell jar. The motor and gearbox are mounted outside the vacuum bell jar, and the output shaft of the gearbox is connected to the damper via a torque load cell and a vacuum rotary feedthrough. The load cell provides measurements of the time-varying responsive damping torque, so that decreases in damping torque associated with incidence of bubbles and the recovery of damping torque after passage of bubbles can be studied in detail. Optionally, an x-ray camera can be used for visual observation of bubbles.

In the original application, the V-DIAPER was not used only to investigate the effects of bubbles; it was also used to confirm the effectiveness of corrective measures that were undertaken in an effort to eliminate bubbles. These measures consisted mostly of improvements in the techniques for filling and sealing the dampers.

This work was done by Brian Ottens and Alphonso Stewart of **Goddard Space Flight Center**. *Further information is contained in a TSP [see page 1].*

GSC-14093

Books and Reports

Development of Gear Technology and Theory of Gearing

A NASA Reference Publication discusses gear technology from mathematical and historical perspectives. Following a preface containing historical and philosophical observations, the first of three chapters presents mathematical details of the theory of gearing, including recent developments attributable to the author and others. The second chapter discusses the development of gear geometry and technology, with emphasis on modifications of gear geometries to improve conditions of meshing. Special attention is given to low-noise gear drives that exhibit stable contact during meshing and to a predesigned parabolic transmission-error function that can accommodate misalignment during operation without sacrificing the suppression of noise. The third chapter presents biographies of inventors, scientists, and founders of gear companies in order to cred-

it the contributions made by previous innovators and to combine the separate pieces of the history of gear technology and the theory of gearing.

This work was done by Faydor L. Litvin of the University of Illinois at Chicago for **Glenn Research Center.** *To obtain a copy of the publication, "Development of Gear Technology and Theory of Gearing," see TSP's [page 1].*

Inquiries concerning rights for the commercial use of this invention should be addressed to NASA Glenn Research Center, Commercial Technology Office, Attn: Steve Fedor, Mail Stop 4-8, 21000 Brookpark Road, Cleveland, Ohio 44135. Refer to LEW-16702.

Mars Ascent Propulsion System

A report presents an overview of continuing efforts to develop an advanced propulsion system for a spacecraft that would ascend from Mars to bring samples to Earth. The system is required to be smaller and to weigh and cost less, in comparison with a conventionally designed system of equal capability. The development efforts include research on several topics, including the following, which are discussed in the report: (1) warm-gas pressurization subsystems for pushing liquid propellants from supply tanks to engines, (2) lightweight, high-performance rocket engines that burn propellant fluids supplied at temperatures below 0 °C, (3) lightweight tanks for propellants and pressurants, and (4) lightweight flow-control components. Finally, the report describes the latest version of the system, which features a two-stage design with pyrotechnic separation.

This work was done by Carl Guernsey, Barry Nakanzo, Hartwell Long, and Andre Yavrouian of Caltech for **NASA's Jet Propulsion Laboratory.** *To obtain a copy of the report, "Advanced Storable Propulsion Technologies for Low-Cost Mars Sample Return," see TSP's [page 1].*
NPO-20428

BLANK PAGE

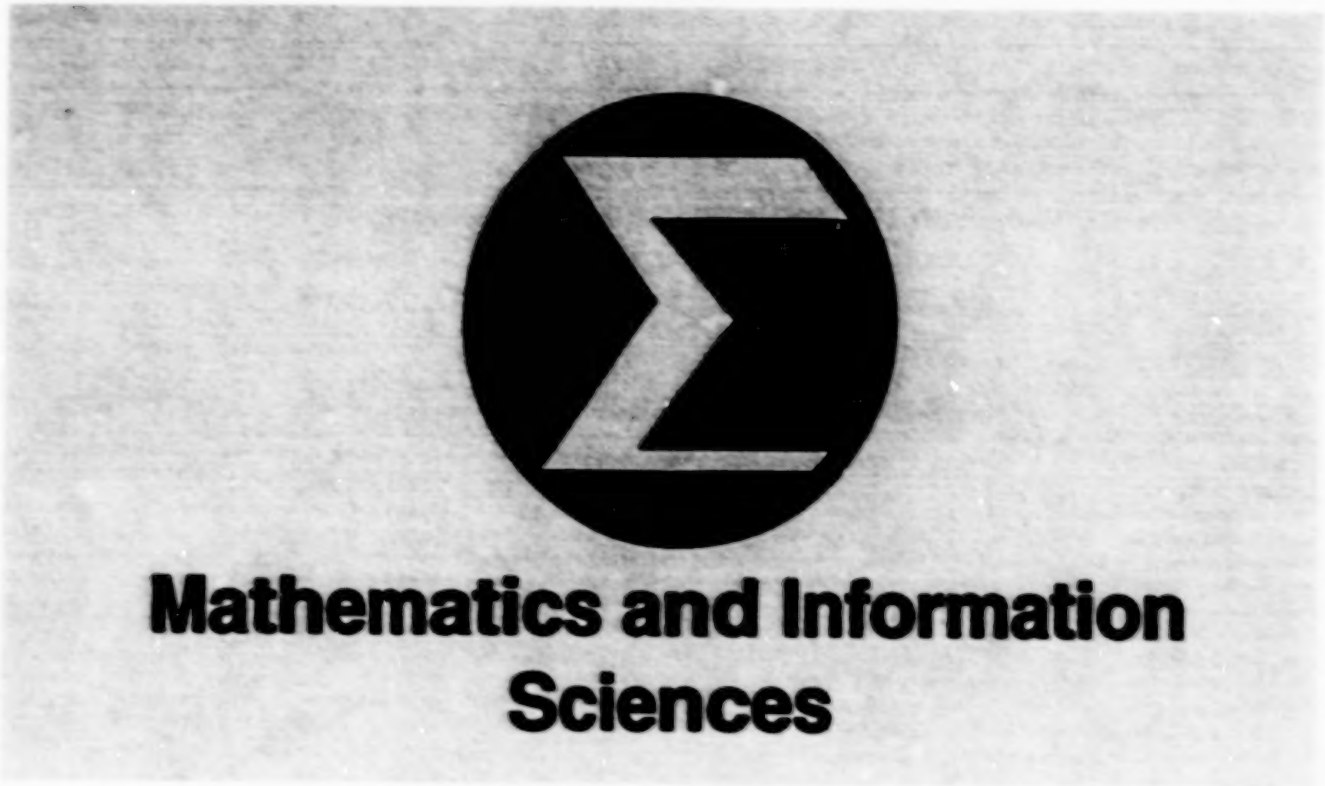

Mathematics and Information Sciences

BLANK PAGE

Automating Work-Time and Attendance Recording on an Intranet

Money is saved through reduction in processing time and prevention of errors.

Goddard Space Flight Center, Greenbelt, Maryland

The OMNI time and attendance system is a workstation software system for automated, centralized recording of work time and attendance, and for flexible scheduling of work by employees in an organization. The OMNI system makes it unnecessary to perform the time-consuming and error-prone tasks of preparing, copying, transporting, or in any other way using or handling paper time cards or other paper records.

Unlike most commercial intranet client/server "groupware" designed for paperless office operations, the OMNI software is not difficult to learn, is not loaded with extra "features" that most organizations do not need, and is compatible with a variety of computers and operating systems. The OMNI software was developed, from the start, to take advantage of popular Web-browser programs (Netscape, Mosaic, and Internet Explorer) installed in many computer workstations.

The OMNI time and attendance software comprises approximately 20 computer scripts in Practical Expression and Report Language (PERL). These scripts run on a Unix workstation that supports a World Wide Web (WWW) server. Preferences can be changed by use of scripts. Administrators can use other scripts to gain access to and to change pertinent information. Supervisors can run still other scripts to obtain summary data and reports.

Employees log into the OMNI system from remote computer terminals and identify themselves to the system by selecting their names and entering passwords. The system responds to each employee by displaying, in a time-card format (see figure), the employee's work-time information as of the most recent previous entry. (This information is recorded in a database maintained by the system.) The employee can update the information by changing job order numbers (referenced by names) and/or numbers of hours worked. The employee can also enter such information as requests for leave and flexible work schedules.

When the employee has finished updating the time-card information, the employee can save the information with or without submitting it for official recording by the system. When the employee submits the information to the system, several things happen:

- The system records the information in the database for retrieval next time.
- By electronic mail, the system sends the electronic equivalent of the employee's time card to a time keeper.

Once the electronic equivalents of time cards from all employees have been received and approved, the information from the databases is printed on time-card stock paper and sent to a payroll-processing system.

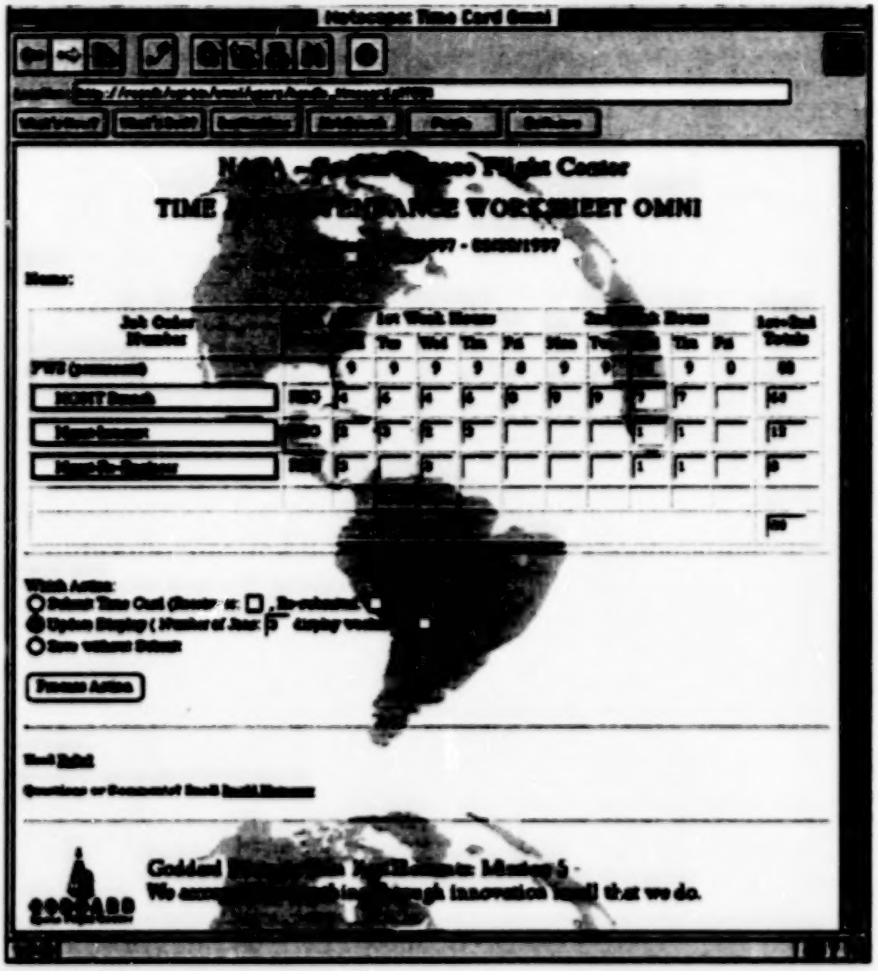

This Example of a Time-Card Entry Page was generated in the OMNI system and displayed by use of Netscape.

Anyone familiar with the World Wide Web can use the OMNI system. Moreover, because the OMNI system runs on an ordinary WWW server on an intranet, it is easily useable in many areas. The performance of the OMNI system for an organization is limited only by the design of the organization's intranet.

In an organization that has a high employee-to-supervisor ratio, the automation of administrative processes by use of OMNI software on an intranet is a quick and inexpensive way to save time across the workplace. For example, in an application to the former Flight Dynamics Systems Branch at Goddard Space Flight Center, the cost of implementing the OMNI system was less than one person-month of effort. Once the OMNI system was in operation, the amount of time spent processing time-card information became 10 minutes per pay period, whereas it took 10 hours per pay period to process time cards in the former paper system. An additional benefit afforded by the OMNI system is an on-line database that can be used to store and track project expenditures by employee; this makes it easier for supervisors to satisfy staffing requirements and to make accurate estimates of future expenditures by project.

This work was done by David Matusow and Joe Spanno of **Goddard Space Flight Center**. *Further information is contained in a TSP [see page 1].*

GSC-13973

Documents on Flight Software for the SAMPEX Spacecraft

A collection of four documents contains information on various aspects of the flight software of the Solar Anomalous and Magnetospheric Particle Explorer (SAMPEX) spacecraft. The first document is part of a longer paper that presents design requirements for the software; the information in this part includes an introduction to the SAMPEX project and a brief description of the Small Explorer Data System (SEDS) — the onboard data-processing system utilizing the software. The second document is a completed form for submittal of the software to NASA's now-discontinued Computer Software Management and Information Center (COSMIC). The third document — apparently an attachment to the COSMIC form — is an outline that briefly describes the purpose, capabilities, and characteristics of the software. The fourth document is a complete paper that describes the software in somewhat more detail: The paper includes a brief historical introduction; an overview of the structure and functions of the software in relation to the SEDS hardware; and discussions of the impact, innovative aspects, and utility of the software.

This work was done by Ray Whitley, R. Hollenhorst, Chuck Clagett, Gil Colon, Jim Watzin, Bruce Savadkin, Mike Blau, Alan Cudmore, Todd Miller, and John Ong of **Goddard Space Flight Center** *and John Allen and Jerry Hengemihle of Dasdalian Systems Corp. To obtain a copy of the collection of documents, see TSP's [page 1].*
GSC-13665

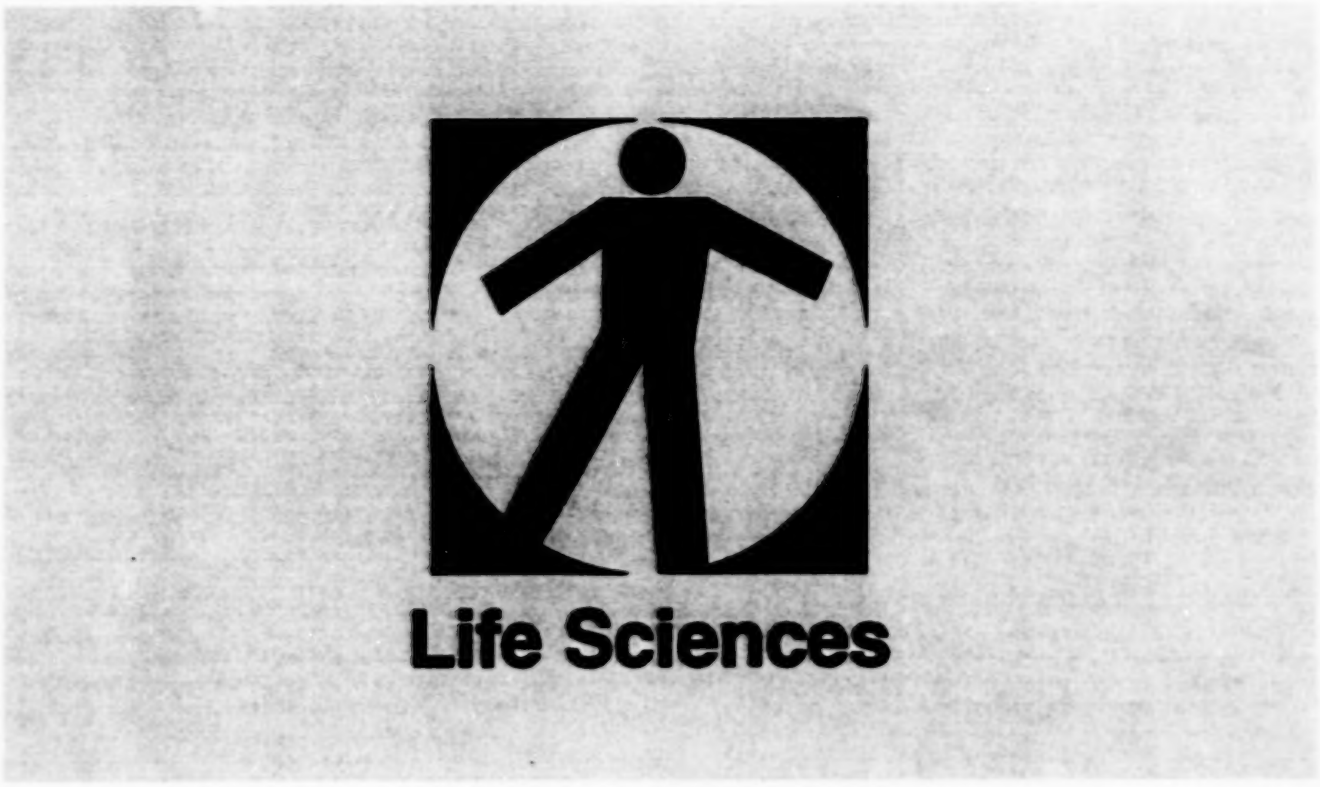

Life Sciences

Hardware, Techniques, and Processes

BLANK PAGE

Wicks for Initiating Hydroponic Growth

These wicks can be reused.

Lyndon B. Johnson Space Center, Houston, Texas

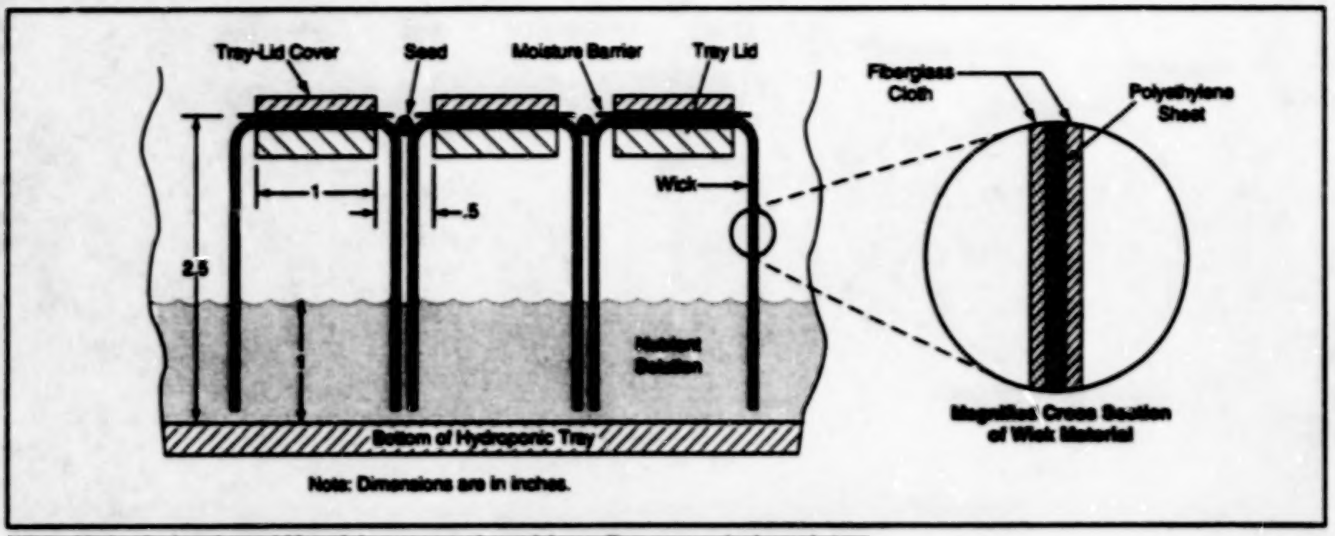

Wicks Made of a Laminated Material support and nourish seedlings over a hydroponic tray.

A material developed for space suits has been found useful in a completely different application: making wicks to support seedlings and to carry water and nutrients to them during the initial stages of hydroponic growth. A modified version of the wick material may also prove useful in wick-based evaporators and humidifiers.

The wick material consists of a middle layer of polyethylene sandwiched between layers of woven glass fibers. The layers are fused together by heating and pressing. Sheets of the material are bent into U-shaped wicks, which are positioned with the tips immersed in an aqueous nutrient solution (see figure). The wick material is chemically inert with respect to the nutrient solution.

Seeds are nested between adjacent wicks. The hydrophilic nature of the fibers and their tight weave ensures wicking of moisture and nutrients to the seeds and, eventually, to the roots. The wicks support roots in the sense that root hairs can cling to the glass fabric, but the tight weave resists penetration by the roots. Seedlings can therefore be removed with little or no damage to the roots, and wicks can be reused.

This work was done by Daniel J. Barta of **Johnson Space Center** *and Robert W. Spaniel of Lockheed Engineering and Sciences Co. Further information is contained in a TSP [see page 1].*

MSC-22539

Portable Device for Chemical Fixation of a Biological Sample

The Kennedy Space Center (KSC) fixation tube is a device for chemical fixation of a biological sample. It is mechanically resilient, small, and easy to use, and is thus well suited to use in the field as well as in the laboratory. Because typical chemical fixatives are extremely hazardous to humans, the device is also designed to contain its fixative solution within a triply-redundantly sealed environment. The device includes a main tube, sample tube, expansion plug, base plug, and top-plug/plunger assembly. Prior to use, the fixative solution is contained at the bottom of the main tube, below the expansion plug. The sample is placed in the sample tube, which is then inserted in the main tube and sealed in the main tube by inserting the top plug. Next, the plunger is used to (1) actuate a mechanism that loosens the seals on the expansion plug, then (2) push the sample tube down against the sample plug, thereby pushing the sample into the fixative solution.

This work was done by Howard William Wells of the Bionetics Corp. and Mark Best of Vector CAD Services for **Kennedy Space Center.**

Inquiries concerning rights for the commercial use of this invention should be addressed to the Technology Programs and Commercialization Office, Kennedy Space Center, (407) 867-6373. Refer to KSC-11993.

END

12-13-99